

Unified Analysis of HetNets using Poisson Cluster Process under Max-Power Association

Chiranjib Saha, Harpreet S. Dhillon, Naoto Miyoshi, and Jeffrey G. Andrews

Abstract

Owing to its flexibility in modeling real-world spatial configurations of users and base stations (BSs), the Poisson cluster process (PCP) has recently emerged as an appealing way to model and analyze heterogeneous cellular networks (HetNets). Despite its undisputed relevance to HetNets – corroborated by the models used in industry – the PCP’s use in performance analysis has been limited. This is primarily because of the lack of analytical tools to characterize performance metrics such as the coverage probability of a user connected to the strongest BS. In this paper, we develop an analytical framework for the evaluation of the coverage probability, or equivalently the complementary cumulative density function (CCDF) of signal-to-interference-and-noise-ratio (SINR), of a typical user in a K -tier HetNet under a max power-based association strategy, where the BS locations of each tier follow either a Poisson point process (PPP) or a PCP. The key enabling step involves conditioning on the parent PPPs of all the PCPs which allows us to express the coverage probability as a product of sum-product and probability generating functionals (PGFLs) of the parent PPPs. In addition to several useful insights, our analysis provides a rigorous way to study the impact of the cluster size on the SINR distribution, which was not possible using existing PPP-based models.

Index Terms

Heterogeneous cellular network, 3GPP, Poisson cluster process, Thomas cluster process, Matérn cluster process.

I. INTRODUCTION

Network heterogeneity is at the heart of current 4G and upcoming 5G networks. A key consequence of the heterogeneous deployments is the emergence of different types of spatial

C. Saha and H. S. Dhillon are with Wireless@VT, Department of ECE, Virginia Tech, Blacksburg, VA, USA. Email: {csaha, hdhillon}@vt.edu. N. Miyoshi is with the Department of Mathematical and Computing Science, Tokyo Institute of Technology, Tokyo, Japan. Email: miyoshi@is.titech.ac.jp. J. G. Andrews is with the Wireless Networking and Communications Group, The University of Texas at Austin, TX, USA. Email: jandrews@ece.utexas.edu.

The support of the US National Science Foundation (Grant CNS-1617896) and Japan Society for the Promotion of Science (JSPS) Grant-in-Aid for Scientific Research (C) 16K00030 is gratefully acknowledged. Last updated: December 6, 2018.

couplings across the locations of BSs and users. Perhaps the most prominent one is the *user-BS coupling*, where the users tend to form spatial clusters or *hotspots* [1]–[3] and small cell BSs (SBSs) are deployed within these hotspots to provide additional capacity. Further, depending on the deployment objectives, the point patterns of BSs of a particular tier may exhibit some *intra-tier coupling*, such as clustering patterns for small cells [4], [5] and repulsive patterns for macrocells deployed under a minimum inter-site distance constraint. Further, *inter-tier coupling* may exist between the locations of BSs of different tiers, for instance, macrocells and small cells when the latter are deployed at the macrocell edge to boost cell edge coverage [6].

Not surprisingly, the HetNet simulation models used by the standardization bodies, such as the third generation partnership project (3GPP), are cognizant of the existence of this spatial coupling [6]. Unfortunately, this is not true for the stochastic geometry based analytical HetNet models, e.g., see [7], [8], which mostly still rely on the assumption that all network elements (BSs and users) are modeled as independent PPPs. That said, it has been recently shown that PCP-based models are well-suited to capture the aforementioned spatial coupling in a similar way as it is incorporated in 3GPP simulation models [1], [9]–[11]. Since PCPs are defined in terms of PPPs, they are also very amenable to mathematical analysis. A key prior work in this area is [1], which completely characterized the downlink coverage probability for a PCP-based HetNet model under max-SINR based association scheme in which the typical user connects to the BS offering maximum *instantaneous* received SINR [1]. However, the downlink analysis for the more practical association scheme in which the typical user connects to the BS offering the strongest received power requires a very different mathematical treatment and is still a key open problem. In this paper, we plug this knowledge gap by providing a complete characterization of coverage probability under this association model.

A. Background and related works

Since the use of PPPs for modeling HetNets is by now fairly well-known, we advise interested readers to refer to books, surveys and tutorials, such as [12]–[16] to learn more about this direction of research. Although sparse, there have been some works on modeling spatial coupling between BSs and users in random spatial models for cellular networks. In [17], user-BS coupling was introduced in a PPP-based single tier cellular network model by conditionally thinning the user PPP and biasing user locations towards the BS locations. Owing to the natural connection of the formation of hotspots to the clustering patterns of PCPs, PCP was used to model the user

distributions in [9], [10], [18], [19], where coupling between the users and BS locations was introduced by placing the SBSs at the cluster centers (parent points) of the user PCP. Further, since intra-tier coupling can be either attractive or repulsive, no single point process is the *best* choice for capturing it. For modeling repulsions, Matérn hard-core process [20], [21], Gauss-Poisson process [22], Strauss hardcore process [23], Ginibre point process [24], [25], and more general determinantal point processes [26] have been used for BS distributions. On the other hand, for modeling attraction, PCP [11] and Geyer saturation process [23] have been proposed. For modeling inter-tier coupling, Poisson hole process (PHP) has been a preferred choice [27], [28], where the macro BSs (MBSs) are modeled as PPP and the SBSs are modeled as another PPP outside the exclusion discs (holes) centered at the MBS locations. Among these “beyond-PPP” spatial models of HetNets, the PCP has attracted significant interest because of its generality in modeling variety of user and BS configurations and its mathematical tractability [1], [29]. We now provide an overview of the existing work on PCP-based models for HetNets.

In [27], [30], the authors assumed that the SBSs in a two-tier HetNet are distributed as a PCP and derived downlink coverage probability assuming that the serving BS is located at a fixed distance from the receiver, which circumvented the need to consider explicit cell association. While this setting provides useful initial insights, the analysis cannot be directly extended to incorporate realistic cell association rules, such as max-power based association [31]. The primary challenge in handling cell association in a stochastic geometry setting is to jointly characterize the serving BS distance and the interference field. This challenge does not appear when BS is assumed to lie at a fixed distance from the receiver, such as in [27], [30]. It is worth noting that the distance of the serving BS from the receiver under max-power based association can be evaluated using contact distance distributions of PCPs, which have recently been characterized in [32], [33]. However, these alone do not suffice because we need to jointly characterize the serving BS distance and the interference field, which is much more challenging. This is the main reason why this problem has remained open for several years. In [34], the authors characterized handoff rates for a typical user following an arbitrary trajectory in a HetNet with PPP and PCP-distributed BSs. Although the setup is very similar to this paper, the metric considered in [34] did not require the characterization of coverage probability. In [35], the authors developed analytical tools to handle this correlation and derived coverage probability when the BSs are modeled as a Matérn cluster process (MCP). However, the analysis is dependent on the geometrical constructions which is very specific to an MCP and is hence not directly applicable

to a general PCP. The coverage analysis for a general PCP was provided in [11] where analytical tractability was preserved by assuming that the SBSs to be operating in a *closed access* mode, i.e, a user can only connect to a SBS of the same cluster. In [1], we have provided a comprehensive coverage analysis for the unified HetNet model under max SINR-based association strategy with SINR threshold greater than unity. However, the analysis cannot be directly extended to the max power-based association setup because of the fundamental difference in the two settings from the analytical perspective. Recently, in [36], the open problem of the coverage analysis for a single tier cellular network under max-power connectivity with PCP-distributed BSs and independent user locations was solved by expressing coverage probability as a sum-product functional over the parent PPP of the BS PCP. Motivated by this novel analytical approach, in this paper we provide the complete coverage analysis for max-power based association strategy for the unified HetNet model introduced in [1].

B. Contributions

We derive the coverage probability of a typical user of a unified K -tier HetNet in which the spatial distributions of K_1 BS tiers are modeled as PCPs and K_2 BS tiers are modeled as PPPs ($K_1 + K_2 = K$). The PCP assumption for the BS tier introduces spatial coupling among the BS locations. We consider two types of users in this network, TYPE 1: users having no spatial coupling with the BSs, and TYPE 2: users whose locations are coupled with the BS locations. For TYPE 1, the user locations are modeled as a stationary point process independent of the BS point processes. For TYPE 2, the coupling between user and BS locations is incorporated by modeling the user locations as a PCP with each user cluster sharing the same cluster center with a BS cluster. The key contributions are highlighted next.

Exact coverage probability analysis. Assuming that a user connects to the BS offering the maximum average received power, we provide an exact analysis of coverage probability for a typical user which is an arbitrarily selected point from the user point process. The key enabler of the coverage probability analysis is a fundamental property of PCP that conditioned on the parent PPP, the PCP can be viewed as an inhomogeneous PPP, which is a relatively more tractable point process compared to PCP. Using this property, we condition on the parent PPPs of all the BS PCPs and derive the conditional coverage probability. Finally, while deconditioning over the parent PPPs, we observe that the coverage probability can be expressed as the product of PGFLs and sum-product functionals of the parent PPPs. This analytical formulation of coverage probability

in terms of known point process functionals over the parent PPPs is the key contribution of the paper and yields an easy-to-compute expression of coverage probability under max-power based association. We then specialize the coverage probability for two instances when the PCPs associated with the BSs are either (i) Thomas cluster process (TCP), where the offspring points are normally distributed around the cluster center, or (ii) MCP, where the offspring points are distributed uniformly at random within a disc centered at the cluster center.

System-level insights. Using the analytical results, we study the impact of spatial parameters such as cluster size, average number of points per cluster and BS density on the coverage probability. Our numerical results demonstrate that the variation of coverage probability with cluster size has conflicting trends for TYPES 1 and 2: for TYPE 1, coverage decreases as cluster size increases, and for TYPE 2, coverage increases as cluster size decreases. As cluster size increases, the coverage probabilities under TYPE 1 and TYPE 2 approach the same limit which is the well-known coverage probability of the PPP-based K -tier HetNet [31], but from two opposite directions. Our numerical results demonstrate that the impact of the variation of cluster size on coverage probability is not as prominent in TYPE 2 as in TYPE 1.

II. SYSTEM MODEL

A. PCP Preliminaries

Before we introduce the proposed PCP-based system model for K -tier HetNet, we provide a formal introduction to PCP.

Definition 1 (Poisson Cluster Process). *A PCP $\Phi(\lambda_p, g, \bar{m})$ in \mathbb{R}^2 can be defined as:*

$$\Phi(\lambda_p, g, \bar{m}) = \bigcup_{\mathbf{z} \in \Phi_p(\lambda_p)} \mathbf{z} + \mathcal{B}^{\mathbf{z}}, \quad (1)$$

where $\Phi_p = \Phi(\lambda_p)$ is the parent PPP with intensity λ_p and $\mathcal{B}^{\mathbf{z}}$ denotes the offspring point process corresponding to a cluster center at $\mathbf{z} \in \Phi_p$ where $\{\mathbf{s} \in \mathcal{B}^{\mathbf{z}}\}$ is an independently and identically distributed (i.i.d.) sequence of random vectors with probability density function (PDF) $g(\mathbf{s})$. The number of points in $\mathcal{B}^{\mathbf{z}}$ is denoted by M , where $M \sim \text{Poisson}(\bar{m})$.

Notation. While we reserve the symbol Φ to denote any point process, to indicate whether it is a PCP or PPP we specify the parameters in parentheses accordingly, i.e., $\Phi(\lambda_p, g, \bar{m})$ denotes a PCP according to Definition 1 and $\Phi(\lambda)$ denotes a PPP with intensity λ .

TABLE I
LIST OF NOTATIONS.

\mathcal{K}	Index set of all BS tiers ($ \mathcal{K} = K$)
$\mathcal{K}_1, \mathcal{K}_2$	Index set of all BS tiers modeled as PCP and PPP
$\Phi_k = \Phi(\lambda_{p_k}, g_k, \bar{m}_k)$	The point process of the k^{th} BS tier, $k \in \mathcal{K}_1$, which is a PCP.
$\Phi_k = \Phi(\lambda_k)$	The point process of the k^{th} BS tier, $k \in \mathcal{K}_2$, which is a PPP.
P_k	Transmit power of a BS in Φ_k
α	Path-loss exponent ($\alpha > 2$)
τ_k	Coverage threshold of Φ_k
$\bar{P}_{j,k}$	$(P_j/P_k)^{1/\alpha}$
$f_{d_k}(\cdot z)$	Conditional PDF of distance of a point of Φ_k ($k \in \mathcal{K}_1$) from origin given its cluster center is located at \mathbf{z} ($z = \ \mathbf{z}\ $)
$f_{c_k}(\cdot), F_{c_k}(\cdot)$	PDF and CDF of contact distance of Φ_k
$\mathcal{C}_{j,k}(r, z)$	$\exp\left(-\bar{m}_k \left(1 - \int_{\bar{P}_{j,k}}^{\infty} \left(1 + \frac{\tau_k P_k r^\alpha}{P_k} y^\alpha\right)^{-1} f_{d_j}(y z) dy\right)\right)$
$\rho(\tau_i, \alpha)$	$1 + \tau_i^{2/\alpha} \int_{\tau_i^{-2/\alpha}}^{\infty} \frac{1}{1+t^{\alpha/2}} dt = 1 + \frac{2\tau_i}{\alpha-2} {}_2\mathcal{F}_1\left[1, 1 - \frac{2}{\alpha}; 2 - \frac{2}{\alpha}; -\tau_i\right]$

A PCP can be viewed as a collection of offspring process \mathcal{B}^z translated by \mathbf{z} for each $\mathbf{z} \in \Phi_p$. Then the sequence of points $\{\mathbf{t}\} \equiv \mathbf{z} + \mathcal{B}^z$ is conditionally i.i.d. with PDF $f(\mathbf{t}|\mathbf{z}) = g(\mathbf{t} - \mathbf{z})$. Note that the conditional distribution of the point coordinates given its cluster center at \mathbf{z} is equivalent to translating a cluster centered at the origin to \mathbf{z} . For a PCP, the following result can be established.

Proposition 1. *Conditioned on the parent point process Φ_p , $\Phi(\lambda_p, g, \bar{m})$ is an inhomogeneous PPP with intensity*

$$\lambda(\mathbf{x}) = \bar{m} \sum_{\mathbf{z} \in \Phi_p} f(\mathbf{x}|\mathbf{z}). \quad (2)$$

Proof: While one can prove this result for a more general setting of Cox processes (see [37]), we prove this result for PCP for completeness as follows. Let N_Φ be the random counting measure associated with the point process Φ . Then, for a Borel set $A \in B(\mathbb{R}^2)$, where $B(\mathbb{R}^2)$ is the Borel σ -algebra on \mathbb{R}^2 , $N_\Phi(A)$ is a random variable denoting the number of points of Φ falling in A . First it is observed that for \mathcal{B}^z , $N_{\mathcal{B}^z}(A) \sim \text{Poisson}(\bar{m} \int_A f(\mathbf{y}|\mathbf{z}) d\mathbf{y})$ since the probability generating function (PGF) of $N_{\mathcal{B}^z}(A)$ is

$$\mathbb{E}[\theta^{N_{\mathcal{B}^z}(A)}] = \mathbb{E}\left[\theta^{\sum_{i=1}^M \mathbf{1}(s_i \in A)}\right] = \mathbb{E}\left[\prod_{i=1}^M \theta^{\mathbf{1}(s_i \in A)}\right] \stackrel{(a)}{=} \mathbb{E}\left[\prod_{i=1}^M \mathbb{E}[\theta^{\mathbf{1}(s_i \in A)}]\right]$$

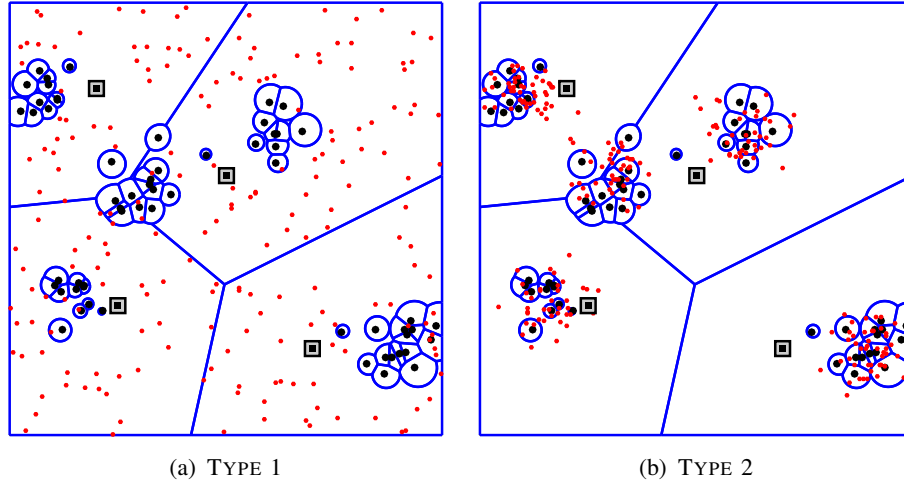


Fig. 1. An illustration of the a two-tier HetNet, where Φ_1 is a PCP of SBSs (illustrated as black dots) and Φ_2 is a PPP of MBSs (illustrated as squares). The users (points of Φ_u) are illustrated as red dots. In (a), Φ_u is a PPP, and in (b), Φ_u is a PCP with the same parent PPP as that of Φ_1 .

$$\stackrel{(b)}{=} \mathbb{E} \left[\prod_{i=1}^M \left(1 - (1 - \theta) \int_A f(\mathbf{y}|\mathbf{z}) d\mathbf{y} \right) \right] = \mathbb{E} \left[\left(1 - (1 - \theta) \int_A f(\mathbf{y}|\mathbf{z}) d\mathbf{y} \right)^M \right]$$

$$\stackrel{(c)}{=} \exp \left(-\bar{m} \int_A f(\mathbf{y}|\mathbf{z}) d\mathbf{y} (1 - \theta) \right).$$

Here (a) follows from the fact that the offspring points are i.i.d. around the cluster center at \mathbf{z} , (b) and (c) are obtained by using the PGF of Bernoulli and Poisson distributions, respectively. Hence $N_{\mathcal{B}^z}(A) \sim \text{Poisson}(\bar{m} \int_A f(\mathbf{y}|\mathbf{z}) d\mathbf{y})$. Now, conditioned on Φ_p the PGF of $N_\Phi(A)$ is expressed as:

$$\mathbb{E}[\theta^{N_\Phi(A)} | \Phi_p] = \mathbb{E} \left[\theta^{\sum_{\mathbf{z} \in \Phi_p} N_{\mathcal{B}^z}(A)} \middle| \Phi_p \right] = \mathbb{E} \left[\prod_{\mathbf{z} \in \Phi_p} \theta^{N_{\mathcal{B}^z}(A)} \middle| \Phi_p \right] \stackrel{(a)}{=} \prod_{\mathbf{z} \in \Phi_p} \mathbb{E} [\theta^{N_{\mathcal{B}^z}(A)} | \Phi_p]$$

$$\stackrel{(b)}{=} \prod_{\mathbf{z} \in \Phi_p} \exp \left(-\bar{m} \int_A f(\mathbf{y}|\mathbf{z}) d\mathbf{y} (1 - \theta) \right) = \exp \left(-\bar{m} \sum_{\mathbf{z} \in \Phi_p} \int_A f(\mathbf{y}|\mathbf{z}) d\mathbf{y} (1 - \theta) \right),$$

where (a) follows from the fact that conditioned on Φ_p , $\{\mathcal{B}^z\}$ is sequence of i.i.d. offspring point processes, (b) is obtained by substituting the PGF of $N_{\mathcal{B}^z}(A)$. Hence it is observed that $N_\Phi(A) | \Phi_p \sim \text{Poisson} \left(\bar{m} \sum_{\mathbf{z} \in \Phi_p} \int_A f(\mathbf{y}|\mathbf{z}) d\mathbf{y} \right)$. Thus $\Phi | \Phi_p$ is an inhomogeneous PPP with intensity measure $\Lambda(A) = \bar{m} \sum_{\mathbf{z} \in \Phi_p} \int_A f(\mathbf{y}|\mathbf{z}) d\mathbf{y}$. ■

B. K -tier HetNet Model

We assume a K -tier HetNet where BSs of each tier are distributed as a PPP or PCP. Let \mathcal{K}_1 and \mathcal{K}_2 denote the index sets of the BS tiers which are modeled as PCP and PPP, respectively, with $|\mathcal{K}_1 \cup \mathcal{K}_2| = K$ and $\mathcal{K}_1 \cap \mathcal{K}_2 = \emptyset$. We denote the point process of the k^{th} BS tier as Φ_k , where Φ_k is either a PCP i.e. $\Phi(\lambda_{p_k}, g_k, \bar{m}_k)$ ($\forall k \in \mathcal{K}_1$) where $\Phi_{p_k} = \Phi(\lambda_{p_k})$ is the parent PPP or a PPP $\Phi(\lambda_k)$ ($\forall k \in \mathcal{K}_2$). Also define $f_k(\mathbf{x}|\mathbf{z}) = g_k(\mathbf{x} - \mathbf{z})$, $\forall k \in \mathcal{K}_1$. Each BS of Φ_k transmits at constant power P_k . We assume that the users are distributed according to a stationary point process Φ_u . We now consider two types of users in the network.

TYPE 1: No user-BS coupling. The first type of users are uniformly distributed over the network, such as, the pedestrians and users in transit, and their locations are independent of the BS locations. There is no restriction on the distribution of these users as long as the distribution is stationary. For instance, one way of modeling the locations of these users is to assume that they are distributed as a homogeneous PPP.

TYPE 2: User-BS coupling. The second type of users are assumed to form spatial clusters (also called *user hotspots*) and their locations can be modeled as a PCP $\Phi_u = \Phi(\lambda_{p_u}, g_u, \bar{m}_u)$ [1], [9]. When the users are clustered, we also assume that one BS tier (say, the q^{th} tier, $q \in \mathcal{K}_1$) is deployed to serve the user hotspots, thus introducing coupling between Φ_u and Φ_q . In other words, Φ_u and Φ_q are two PCPs having same parent PPP $\Phi_{p_q} \equiv \Phi_{p_u}$. Hence conditioned on Φ_{p_q} , Φ_u and Φ_q are (conditionally) independent but not identically distributed. This assumption is motivated by the way SBSs are placed at higher densities in the locations of user hotspots in 3GPP simulation models of HetNets [4], [5].

Remark 1. For TYPE 1, Φ_u can be any general stationary point process including PPP and for TYPE 2, we do not specify \bar{m}_u of Φ_u , since \bar{m}_u does not appear explicitly in the coverage analysis. However, these specifications of Φ_u are required when one has to characterize other metrics like BS load and rate coverage probability [38], [39]. Further, the coverage probability analysis that follows can be extended for a general user distribution which is the superposition of PPP and PCPs along similar lines to [9].

In Fig. 1, we provide an illustration of the system model. For both types of user distributions, we perform our analysis for a *typical* user which corresponds to a point selected uniformly at random from Φ_u . Since Φ_u is stationary, the typical user is assumed to be located at the origin

without loss of generality. For TYPE 1, since Φ_u and $\Phi_k, \forall k \in \mathcal{K}$ are independent, the selection of the typical user does not bias the distribution of Φ_k . However, for TYPE 2, the selection of the typical user affects the BS point process Φ_q due to the existence of user-BS coupling. We assume that the typical user belongs to a cluster centered at \mathbf{z}_0 . By construction, Φ_q is always conditioned to have a cluster centered at \mathbf{z}_0 . Hence, the typical user will *see* the palm version of Φ_q which, by Slivnyak's theorem, is equivalent to the superposition of Φ_q and $\mathbf{z}_0 + \mathcal{B}^{\mathbf{z}_0}$ where Φ_q and $\mathbf{z}_0 + \mathcal{B}^{\mathbf{z}_0}$ are independent. For TYPE 2, we modify Φ_q as $\Phi_q = \Phi(\lambda_{p_q}, g_q, \bar{m}_q) \cup \mathbf{z}_0 + \mathcal{B}^{\mathbf{z}_0}$. Consequently, the underlying parent point process is modified as $\Phi_{p_q} = \Phi(\lambda_{p_q}) \cup \{\mathbf{z}_0\}$. The BS cluster $\mathcal{B}^{\mathbf{z}_0}$ is termed as the *representative cluster*.

Considering the typical user at origin, the downlink power received from a BS at $\mathbf{x} \in \Phi_k$ is expressed as $P_k h_{\mathbf{x}} \|\mathbf{x}\|^{-\alpha}$, where $h_{\mathbf{x}}$ and α denote the small scale fading and path-loss exponent, respectively. We assume that each link undergoes Rayleigh fading, hence $\{h_{\mathbf{x}}\}$ is a sequence of i.i.d. random variables with $h_{\mathbf{x}} \sim \exp(1)$. The user connects to the BS providing the maximum received power averaged over fading. Thus, if \mathbf{x}^* is the location of the serving BS, then, $\mathbf{x}^* = \arg \max_{\{\tilde{\mathbf{x}}_k, k \in \mathcal{K}\}} P_k \|\tilde{\mathbf{x}}_k\|^{-\alpha}$, where $\tilde{\mathbf{x}}_k = \arg \max_{\mathbf{x} \in \Phi_k} P_k \|\mathbf{x}\|^{-\alpha} = \arg \min_{\mathbf{x} \in \Phi_k} \|\mathbf{x}\|$ is the location of candidate serving BS in Φ_k . Note that the candidate serving BS in Φ_k is the BS in Φ_k which is geometrically closest to the user. We first define the *association event* corresponding to the i^{th} tier as the event that the serving BS belongs to Φ_i , denoted as $\mathcal{S}_i = \{\mathbf{x}^* = \tilde{\mathbf{x}}_i\}$. Conditioned on \mathcal{S}_i , the SINR experienced by the typical user is

$$\text{SINR}(\mathbf{x}^*) = \frac{P_i h_{\mathbf{x}^*} \|\mathbf{x}^*\|^{-\alpha}}{N_0 + \sum_{j \in \mathcal{K}} \sum_{\mathbf{x} \in \Phi_j \setminus \{\mathbf{x}^*\}} P_j h_{\mathbf{x}} \|\mathbf{x}\|^{-\alpha}}, \quad (3)$$

where N_0 is the thermal noise power. We define the coverage probability as the probability of the union of K mutually exclusive coverage events

$$P_c = \mathbb{P} \left(\bigcup_{i \in \mathcal{K}} \{\text{SINR}(\mathbf{x}^*) > \tau_i, \mathcal{S}_i\} \right) = \sum_{i \in \mathcal{K}} \mathbb{P}(\text{SINR}(\mathbf{x}^*) > \tau_i, \mathcal{S}_i), \quad (4)$$

where we call the i^{th} term under the summation as the i^{th} *tier coverage probability* which is the joint probability of the events \mathcal{S}_i and $\{\text{SINR}(\mathbf{x}^*) > \tau_i\}$. Here τ_i is the SINR threshold for the i^{th} tier required for successful demodulation and decoding of the received signal.

III. COVERAGE PROBABILITY ANALYSIS

We begin our coverage analysis by first conditioning on every parent PPP, i.e., $\Phi_{p_k}, \forall k \in$

\mathcal{K}_1 . Following Proposition 1, $\Phi_k|\Phi_{p_k}$ will be inhomogeneous PPP with intensity $\lambda_k(\mathbf{x}) = \bar{m}_k \sum_{\mathbf{z} \in \Phi_{p_k}} f_k(\mathbf{x}|\mathbf{z})$. A slightly different situation occurs for Φ_q in TYPE 2. However, once Φ_{p_q} is modified by adding a point at \mathbf{z}_0 to the original parent PPP, $\Phi_q|\Phi_{p_q}$ again becomes an inhomogeneous PPP with intensity $\bar{m}_q \sum_{\mathbf{z} \in \Phi_{p_q} \cup \{\mathbf{z}_0\}} f_q(\mathbf{x}|\mathbf{z})$.

Notation. To denote the distance of a point $\mathbf{y} \in \mathbb{R}^2$, we use y and $\|\mathbf{y}\|$ interchangeably.

A. Contact Distance Distribution

First we will derive the distribution of $\|\tilde{\mathbf{x}}_k\|$, $k \in \mathcal{K}$, or the distance distribution of the candidate serving BS of tier k . Since $\|\tilde{\mathbf{x}}_k\|$ is the nearest BS to the typical user which is at origin, the distribution of $\|\tilde{\mathbf{x}}_k\|$ is the same as the contact distance distribution of Φ_k , denoted as $f_{c_k}(r|\Phi_{p_k})$. Let $f_{d_k}(r|\mathbf{z})$ and $F_{d_k}(r|\mathbf{z})$ denote the PDF and CDF of the distance of a randomly selected point of Φ_k ($k \in \mathcal{K}_1$) given its cluster center is located at \mathbf{z} . Before presenting the contact distance distributions, we observe the following property of the conditional distance distribution.

Lemma 1. *If the offspring points are isotropically distributed around the cluster center i.e., the radial coordinates of the offspring points with respect to the cluster center have the joint PDF $g_k(s, \theta_s) = g_{k(1)}(s) \frac{1}{2\pi}$, where $g_{k(1)}(\cdot)$ is the marginal PDF of the radial coordinate, then, $f_{d_k}(r|\mathbf{z}) = f_{d_k}(r|z)$ and $F_{d_k}(r|\mathbf{z}) = F_{d_k}(r|z)$. That is, the conditional distance distribution depends only on the magnitude of \mathbf{z} .*

Proof: Let $\mathbf{x} \in \Phi_k$ is the location of the point whose cluster center is located at \mathbf{z} . Then,

$$\begin{aligned} F_{d_k}(r|\mathbf{z}) &= \mathbb{P}(\|\mathbf{x}\| < r|\mathbf{z}) = \int_{b(\mathbf{0}, r)} g_k(\mathbf{x} - \mathbf{z}) d\mathbf{x} \\ &= \int_0^{2\pi} \frac{1}{2\pi} \int_0^r g_{k(1)}(\sqrt{x^2 + z^2 - 2xz \cos(\theta_x - \theta_z)}) x dx d\theta_x \\ &= \int_{\theta_z}^{2\pi + \theta_z} \frac{1}{2\pi} \int_0^r g_{k(1)}(\sqrt{x^2 + z^2 - 2xz \cos \theta}) x dx d\theta. \end{aligned}$$

Here $b(\mathbf{0}, r)$ denotes a disc of radius r centered at the origin. Differentiating with respect to r ,

$$f_{d_k}(r|\mathbf{z}) = \int_{\theta_z}^{2\pi + \theta_z} \frac{1}{2\pi} g_{k(1)}(\sqrt{r^2 + z^2 - 2rz \cos \theta}) r d\theta. \quad (5)$$

Since the region of the integral over θ is the perimeter of the disc $b(\mathbf{0}, z)$, it is independent of

the choice of θ_z . ■

We now characterize the PDF of $\|\tilde{\mathbf{x}}_k\|$.

Lemma 2. For $k \in \mathcal{K}_1$, conditioned on $\Phi_{\mathbf{p}_k}$, the PDF and CDF of $\|\tilde{\mathbf{x}}_k\|$ are given as:

$$f_{c_k}(r|\Phi_{\mathbf{p}_k}) = \bar{m}_k \sum_{\mathbf{z} \in \Phi_{\mathbf{p}_k}} f_{d_k}(r|z) \prod_{\mathbf{z} \in \Phi_{\mathbf{p}_k}} \exp(-\bar{m}_k F_{d_k}(r|z)), \quad r \geq 0, \quad (6)$$

and

$$F_{c_k}(r|\Phi_{\mathbf{p}_k}) = 1 - \exp\left(-\bar{m}_k \sum_{\mathbf{z} \in \Phi_{\mathbf{p}_k}} \int_0^r f_{d_k}(y|z) dy\right), \quad r \geq 0. \quad (7)$$

Proof: For $k \in \mathcal{K}_1$, the CDF of $\|\tilde{\mathbf{x}}_k\|$ is

$$\begin{aligned} F_{c_k}(r|\Phi_{\mathbf{p}_k}) &= 1 - \mathbb{P}(\Phi(b(\mathbf{0}, r)) = 0 | \Phi_{\mathbf{p}_k}) \\ &= 1 - \exp\left(-\int_{b(\mathbf{0}, r)} \lambda_k(\mathbf{x}) d\mathbf{x}\right) \\ &= 1 - \exp\left(-\bar{m}_k \sum_{\mathbf{z} \in \Phi_{\mathbf{p}_k} \cap b(\mathbf{0}, r)} \int f_k(\mathbf{y}|\mathbf{z}) d\mathbf{y}\right) \\ &= 1 - \exp\left(-\bar{m}_k \sum_{\mathbf{z} \in \Phi_{\mathbf{p}_k}} \int_0^r f_{d_k}(y|z) dy\right). \end{aligned}$$

The last step is due the fact that integrating a joint PDF of polar coordinates over $b(\mathbf{0}, r)$ is equivalent to integrating the marginal PDF of radial coordinate over $(0, r]$. The final result in (6) can be obtained by differentiating the CDF with respect to r . ■

Note that one can obtain the PDF of the contact distance of PCP by deconditioning $f_{c_k}(r|\Phi_{\mathbf{p}_k})$ over $\Phi_{\mathbf{p}_k}$ [36]. This is an alternative approach to the one presented in [32], [33] for the derivation of contact distance distribution of PCP.

When Φ_k is a PPP, i.e., $k \in \mathcal{K}_2$, the distribution of $\|\tilde{\mathbf{x}}_k\|$ is the well-known Rayleigh distribution, given by:

$$f_{c_k}(r) = 2\pi\lambda_k r \exp(-\pi\lambda_k r^2), \quad F_{c_k}(r) = 1 - \exp(-\pi\lambda_k r^2), \quad r \geq 0. \quad (8)$$

B. Association Probability and Serving Distance Distribution

We define association probability to the i^{th} tier as $\mathbb{P}(\mathcal{S}_i)$. The association probability is derived as follows.

Lemma 3. *Conditioned on $\Phi_{p_k}, \forall k \in \mathcal{K}_1$, the association probability to the i^{th} tier is given by:*

$$\mathbb{P}(\mathcal{S}_i | \Phi_{p_k}, \forall k \in \mathcal{K}_1) =$$

$$\bar{m}_i \int_0^\infty \sum_{\mathbf{z} \in \Phi_{p_i}} f_{d_i}(r|z) \prod_{j_1 \in \mathcal{K}_1} \prod_{\mathbf{z} \in \Phi_{p_{j_1}}} \exp(-\bar{m}_{j_1} F_{d_{j_1}}(\bar{P}_{j_1, i} r | z)) \prod_{j_2 \in \mathcal{K}_2} \exp(-\pi \lambda_{j_2} \bar{P}_{j_2, i}^2 r^2) dr, \quad \text{if } i \in \mathcal{K}_1, \quad (9a)$$

$$2\pi \lambda_i \int_0^\infty \prod_{j_1 \in \mathcal{K}_1} \prod_{\mathbf{z} \in \Phi_{p_{j_1}}} \exp(-\bar{m}_{j_1} F_{d_{j_1}}(\bar{P}_{j_1, i} r | z)) \prod_{j_2 \in \mathcal{K}_2} \exp(-\pi \lambda_{j_2} \bar{P}_{j_2, i}^2 r^2) r dr, \quad \text{if } i \in \mathcal{K}_2, \quad (9b)$$

where $\bar{P}_{j, i} = (P_j / P_i)^{1/\alpha}$.

Proof: See Appendix A. ■

We now derive the PDF of the conditional serving distance i.e. $\|\mathbf{x}^*\|$ given \mathcal{S}_i and $\Phi_{p_k}, \forall k \in \mathcal{K}_1$.

Lemma 4. *The PDF of $\|\mathbf{x}^*\|$ conditioned on association to the i^{th} tier and $\Phi_{p_k}, \forall k \in \mathcal{K}_1$ is given as: $f_{s_i}(r | \mathcal{S}_i, \Phi_{p_k}, \forall k \in \mathcal{K}_1) =$*

$$\frac{\bar{m}_i}{\mathbb{P}(\mathcal{S}_i | \Phi_{p_k}, \forall k \in \mathcal{K}_1)} \sum_{\mathbf{z} \in \Phi_{p_i}} f_{d_i}(r|z) \prod_{j_1 \in \mathcal{K}_1} \prod_{\mathbf{z} \in \Phi_{p_{j_1}}} \exp(-\bar{m}_{j_1} F_{d_{j_1}}(\bar{P}_{j_1, i} r | z)) \times \prod_{j_2 \in \mathcal{K}_2} \exp(-\pi \lambda_{j_2} \bar{P}_{j_2, i}^2 r^2), \quad r \geq 0, \quad \text{if } i \in \mathcal{K}_1, \quad (10a)$$

$$\frac{2\pi \lambda_i}{\mathbb{P}(\mathcal{S}_i | \Phi_{p_k}, \forall k \in \mathcal{K}_1)} \prod_{j_1 \in \mathcal{K}_1} \prod_{\mathbf{z} \in \Phi_{p_{j_1}}} \exp(-\bar{m}_{j_1} F_{d_{j_1}}(\bar{P}_{j_1, i} r | z)) \prod_{j_2 \in \mathcal{K}_2} \exp(-\pi \lambda_{j_2} \bar{P}_{j_2, i}^2 r^2) r, \quad r \geq 0, \quad \text{if } i \in \mathcal{K}_2. \quad (10b)$$

Proof: See Appendix B. ■

C. Coverage Probability

Before deriving the main results on coverage probability, we first introduce PGFL and sum-product functional of a point process which will be appearing repeatedly into the coverage analysis.

Definition 2 (PGFL). *PGFL of a point process Φ is defined as: $\mathbb{E} \left[\prod_{\mathbf{x} \in \Phi} \mu(\mathbf{x}) \right]$, where $\mu(\mathbf{x}) :$*

$\mathbb{R}^2 \rightarrow [0, 1]$ is measurable.

Lemma 5. When $\Phi(\lambda(\mathbf{x}))$ is a PPP, the PGFL is given as [37]:

$$\mathbb{E} \left[\prod_{\mathbf{x} \in \Phi} \mu(\mathbf{x}) \right] = \exp \left(- \int_{\mathbb{R}^2} \lambda(\mathbf{x})(1 - \mu(\mathbf{x})) d\mathbf{x} \right). \quad (11)$$

When $\mu(\mathbf{x}) = \mu(x)$ and $\Phi(\lambda)$ is homogeneous, then (11) becomes:

$$\mathbb{E} \left[\prod_{\mathbf{y} \in \Phi} \mu(y) \right] = \exp \left(-2\pi\lambda \int_0^\infty (1 - \mu(y))y dy \right). \quad (12)$$

Definition 3 (Sum-product functional). *Sum-product functional of a point process Φ is defined in this paper as $\mathbb{E} \left[\sum_{\mathbf{x} \in \Phi} \nu(\mathbf{x}) \prod_{\mathbf{y} \in \Phi} \mu(\mathbf{y}) \right]$, where $\nu(\mathbf{x}) : \mathbb{R}^2 \rightarrow \mathbb{R}^+$ and $\mu(\mathbf{y}) : \mathbb{R}^2 \rightarrow [0, 1]$ are measurable.*

For a PPP, the sum-product functional is given by the following Lemma.

Lemma 6. When $\Phi(\lambda(\mathbf{x}))$ is a PPP, the sum-product functional is given as [1], [40]

$$\mathbb{E} \left[\sum_{\mathbf{x} \in \Phi} \nu(\mathbf{x}) \prod_{\mathbf{y} \in \Phi} \mu(\mathbf{y}) \right] = \int_{\mathbb{R}^2} \lambda(\mathbf{x})\nu(\mathbf{x})\mu(\mathbf{x})d\mathbf{x} \exp \left(- \int_{\mathbb{R}^2} \lambda(\mathbf{y})(1 - \mu(\mathbf{y}))d\mathbf{y} \right). \quad (13)$$

When $\nu(\mathbf{x}) \equiv \nu(x)$, $\mu(\mathbf{x}) \equiv \mu(x)$, and $\Phi(\lambda)$ is homogeneous, then (13) becomes:

$$\mathbb{E} \left[\sum_{\mathbf{x} \in \Phi} \nu(x) \prod_{\mathbf{y} \in \Phi} \mu(y) \right] = 2\pi\lambda \int_0^\infty \nu(x)\mu(x)x dx \exp \left(-2\pi\lambda \int_0^\infty (1 - \mu(y))y dy \right). \quad (14)$$

Before providing the final expression of coverage probability, we provide an important intermediate expression of the conditional i^{th} tier coverage probability given all parent point processes. In fact, a key contribution of this paper, as will be evident in sequel, is to show that this conditional coverage probability can be factored as a product of standard functionals (such as PGFL and sum-product functional) of the parent PPPs.

Lemma 7. *The i^{th} tier coverage probability given $\Phi_{p_k}, \forall k \in \mathcal{K}_1$ is given by $\mathbb{P}(\text{SINR}(\mathbf{x}^*) > \tau_i, \mathcal{S}_i | \Phi_{p_k}, \forall k \in \mathcal{K}_1) =$*

$$\bar{m}_i \int_0^\infty \exp\left(-\frac{\tau_i N_0 r^\alpha}{P_i}\right) \prod_{j_1 \in \mathcal{K}_1 \setminus \{i\}} \prod_{\mathbf{z} \in \Phi_{p_{j_1}}} \mathcal{C}_{j_1,i}(r, z) \prod_{j_2 \in \mathcal{K}_2} \exp(-\pi r^2 \lambda_{j_2} \bar{P}_{j_2,i}^2 \rho(\tau_i, \alpha)) \times \left(\sum_{\mathbf{z} \in \Phi_{p_i}} f_{d_i}(r|z) \prod_{\mathbf{z} \in \Phi_{p_i}} \mathcal{C}_{i,i}(r, z) \right) dr, \text{ when } i \in \mathcal{K}_1, \quad (15a)$$

$$2\pi \lambda_i \int_0^\infty \exp\left(-\frac{\tau_i N_0 r^\alpha}{P_i}\right) \prod_{j_1 \in \mathcal{K}_1} \prod_{\mathbf{z} \in \Phi_{p_{j_1}}} \mathcal{C}_{j_1,i}(r, z) \prod_{j_2 \in \mathcal{K}_2} \exp(-\pi r^2 \lambda_{j_2} \bar{P}_{j_2,i}^2 \rho(\tau_i, \alpha)) r dr, \text{ when } i \in \mathcal{K}_2, \quad (15b)$$

where

$$\mathcal{C}_{j,k}(r, z) = \exp\left(-\bar{m}_j \left(1 - \int_{\bar{P}_{j,k} r}^\infty \frac{f_{d_j}(y|z)}{1 + \tau_k \frac{(\bar{P}_{j,k} r)^\alpha}{y^\alpha}} dy\right)\right), \quad (16)$$

and, $\rho(\tau_i, \alpha) = 1 + \tau_i^{2/\alpha} \int_{\tau_i^{-2/\alpha}}^\infty \frac{1}{1+t^{\alpha/2}} dt = \frac{2\tau_i}{\alpha-2} {}_2\mathcal{F}_1\left[1, 1 - \frac{2}{\alpha}; 2 - \frac{2}{\alpha}; -\tau_i\right]$, where ${}_2\mathcal{F}_1$ is the Gauss hypergeometric function [31].

Proof: See Appendix C. ■

Looking closely at the expressions of the i^{th} tier coverage probability given $\Phi_{p_k}, \forall k \in \mathcal{K}_1$, we find two terms: (i) $\prod_{\mathbf{z} \in \Phi_{p_{j_1}}} \mathcal{C}_{j_1,i}(r, z)$ in (15a) and (15b), and (ii) $\sum_{\mathbf{z} \in \Phi_{p_i}} f_{d_i}(r|z) \prod_{\mathbf{z} \in \Phi_{p_i}} \mathcal{C}_{i,i}(r, z)$ in (15a). These two terms are respectively product and sum-product over all points of Φ_{p_k} which will be substituted by the PGFL and sum-product functional of Φ_{p_k} while deconditioning over Φ_{p_k} .

Remark 2. In order to apply PGFL and sum-product functional expressions of PPP given by (12) and (14), respectively, we require the condition: $\int_0^\infty \log(|\mathcal{C}_{j_1,i}(r, z)|) z dz < \infty, \forall j_1 \in \mathcal{K}_1$. In [36, Appendix B], it was shown that this condition always holds for the form of $\mathcal{C}_{j_1,i}(r, z)$ given by (16).

Until this point, all results were conditioned on $\Phi_{p_k}, \forall k \in \mathcal{K}_1$. Remember that in Section II-B, we introduced two types of spatial interaction between the users and BSs. Since, by construction, these two types differ only in Φ_{p_q} for some $q \in \mathcal{K}_1$, we were able to treat TYPE 1 and TYPE 2 within the same analytical framework. We now present the final expression of P_c for the two types explicitly by deconditioning the conditional coverage probability over $\Phi_{p_k}, \forall k \in \mathcal{K}_1$ in

the following Theorems.

Theorem 1 (TYPE 1). *The coverage probability is given as:*

$$P_c = \sum_{i=1}^K \mathbb{P}(\text{SINR} > \tau_i, \mathcal{S}_i), \quad (17)$$

where, the i^{th} tier coverage probability, $\mathbb{P}(\text{SINR} > \tau_i, \mathcal{S}_i) =$

$$2\pi \lambda_{p_i} \bar{m}_i \int_0^\infty \exp\left(-\frac{\tau_i N_0 r^\alpha}{P_i}\right) \prod_{j_1 \in \mathcal{K}_1} \exp\left(-2\pi \lambda_{p_{j_1}} \int_0^\infty (1 - \mathcal{C}_{j_1,i}(r, z)) z dz\right) \times \\ \exp\left(-\pi r^2 \sum_{j_2 \in \mathcal{K}_2} \lambda_{j_2} \bar{P}_{j_2,i}^2 \rho(\tau_i, \alpha)\right) \int_0^\infty f_{d_i}(r|z) \mathcal{C}_{i,i}(r, z) z dz dr, \text{ for } i \in \mathcal{K}_1, \quad (18a)$$

$$2\pi \lambda_i \int_0^\infty \exp\left(-\frac{\tau_i N_0 r^\alpha}{P_i}\right) \prod_{j_1 \in \mathcal{K}_1} \exp\left(-2\pi \lambda_{p_{j_1}} \int_0^\infty (1 - \mathcal{C}_{j_1,i}(r, z)) z dz\right) \times \\ \exp\left(-\pi r^2 \sum_{j_2 \in \mathcal{K}_2} \lambda_{j_2} \bar{P}_{j_2,i}^2 \rho(\tau_i, \alpha)\right) r dr, \text{ for } i \in \mathcal{K}_2. \quad (18b)$$

Proof: When $i \in \mathcal{K}_1$, we get from (15a), $\mathbb{P}(\text{SINR} > \tau_i, \mathcal{S}_i) = \mathbb{E}[\mathbb{P}(\text{SINR} > \tau_i, \mathcal{S}_i | \Phi_{p_k}, \forall k \in \mathcal{K}_1)] =$

$$\bar{m}_i \int_0^\infty \exp\left(-\frac{\tau_i N_0 r^\alpha}{P_i}\right) \prod_{j_1 \in \mathcal{K}_1 \setminus \{i\}} \mathbb{E}_{\Phi_{p_{j_1}}} \left[\prod_{\mathbf{z} \in \Phi_{p_{j_1}}} \mathcal{C}_{j_1,i}(r, z) \right] \exp\left(-\pi r^2 \sum_{j_2 \in \mathcal{K}_2} \lambda_{j_2} \bar{P}_{j_2,i}^2 \rho(\tau_i, \alpha)\right) \times \\ \mathbb{E}_{\Phi_{p_i}} \left[\sum_{\mathbf{z} \in \Phi_{p_i}} f_{d_i}(r|z) \prod_{\mathbf{z} \in \Phi_{p_i}} \mathcal{C}_{i,i}(r, z) \right] dr.$$

This step is enabled by the assumption that Φ_j -s are independent $\forall j \in \mathcal{K}$. The final expression is obtained by substituting the PGFL of Φ_{p_k} for $k \in \mathcal{K}_1 \setminus \{i\}$ from (12) and the sum-product functional of Φ_{p_i} from (14). The final expression follows from some algebraic simplifications.

Now, for $i \in \mathcal{K}_2$, from (15b), we get

$$\mathbb{P}(\text{SINR} > \tau_i, \mathcal{S}_i) = 2\pi \lambda_i \int_0^\infty \exp\left(-\frac{\tau_i N_0 r^\alpha}{P_i}\right) \prod_{j_1 \in \mathcal{K}_1} \mathbb{E}_{\Phi_{p_{j_1}}} \left[\prod_{\mathbf{z} \in \Phi_{p_{j_1}}} \mathcal{C}_{j_1,i}(r, z) \right] \times \\ \exp\left(-\pi r^2 \sum_{j_2 \in \mathcal{K}_2} \lambda_{j_2} \bar{P}_{j_2,i}^2 \rho(\tau_i, \alpha)\right) r dr.$$

We then use the PGFL of $\Phi_{p_{j_1}}$ from (12) to obtain the final expression. \blacksquare

Theorem 2 (TYPE 2). *The coverage probability P_c can be written as (17), where the i^{th} tier coverage probability is: $\mathbb{P}(\text{SINR} > \tau_i, \mathcal{S}_i) =$*

$$2\pi\lambda_{p_i}\bar{m}_i \int_0^\infty \exp\left(-\frac{\tau_i N_0 r^\alpha}{P_i}\right) \prod_{j_1 \in \mathcal{K}_1} \exp\left(-2\pi\lambda_{p_{j_1}} \int_0^\infty (1 - \mathcal{C}_{j_1,i}(r, z)) z dz\right) \int_0^\infty \mathcal{C}_{q,i}(r, z_0) f_{d_u}(z_0|0) dz_0 \times \\ \exp\left(-\pi r^2 \sum_{j_2 \in \mathcal{K}_2} \lambda_{j_2} \bar{P}_{j_2,i}^2 \rho(\tau_i, \alpha)\right) \int_0^\infty f_{d_i}(r|z) \mathcal{C}_{i,i}(r, z) z dz dr, \text{ for } i \in \mathcal{K}_1 \setminus \{q\}, \quad (19a)$$

$$\bar{m}_q \int_0^\infty \exp\left(-\frac{\tau_i N_0 r^\alpha}{P_q}\right) \prod_{j_1 \in \mathcal{K}_1} \exp\left(-2\pi\lambda_{p_{j_1}} \int_0^\infty (1 - \mathcal{C}_{j_1,i}(r, z)) z dz\right) \exp\left(-\pi r^2 \sum_{j_2 \in \mathcal{K}_2} \lambda_{j_2} \bar{P}_{j_2,q}^2 \rho(\tau_q, \alpha)\right) \times \\ \left(\int_0^\infty f_{d_q}(r|z_0) \mathcal{C}_{q,q}(r, z_0) f_{d_u}(z_0|0) dz_0 + 2\pi\lambda_{p_q} \int_0^\infty f_{d_q}(r|z) \mathcal{C}_{q,q}(r, z) z dz \times \right. \\ \left. \int_0^\infty \mathcal{C}_{q,q}(r, z_0) f_{d_u}(z_0|0) dz_0 \right) dr, \text{ for } i = q, \quad (19b)$$

$$2\pi\lambda_i \int_0^\infty \exp\left(-\frac{\tau_i N_0 r^\alpha}{P_i}\right) \prod_{j_1 \in \mathcal{K}_1} \exp\left(-2\pi\lambda_{p_{j_1}} \int_0^\infty (1 - \mathcal{C}_{j_1,i}(r, z)) z dz\right) \times \\ \int_0^\infty \mathcal{C}_{q,i}(r, z_0) f_{d_u}(z_0|0) dz_0 \exp\left(-\pi r^2 \sum_{j_2 \in \mathcal{K}_2} \lambda_{j_2} \bar{P}_{j_2,i}^2 \rho(\tau_i, \alpha)\right) r dr, \text{ for } i \in \mathcal{K}_2. \quad (19c)$$

Here $f_{d_u}(z_0|0)$ denotes the distance distribution of a point of Φ_u from its cluster center which resides at origin.

Proof: See Appendix D. \blacksquare

We conclude this discussion with the following remark.

Remark 3. *The analytical framework developed in this Section provisions to model the k^{th} BS tier, where $k \in \mathcal{K}_1$ as any arbitrary PCP $\Phi(\lambda_{p_k}, g_k, \bar{m}_k)$. By looking into the expressions of P_c in Theorems 1 and 2, it is apparent that given K_1 PCPs with arbitrary distributions, i.e., $\{\Phi_k = \Phi(\lambda_{p_k}, g_k, \bar{m}_k), k \in \mathcal{K}_1\}$, the only non-trivial step is to find the conditional distance*

distributions $\{f_{d_k}(x|z)\}$ which need to be simply plugged into the expressions of $\mathbb{P}(\text{SINR} > \tau_i, \mathcal{S}_i)$ in (18)-(19).

The unified model discussed in this paper reduces to the conventional PPP-based HetNet model with no spatial coupling between users and BS locations by setting $\mathcal{K}_1 = \emptyset$. For this scenario, TYPE 2 becomes irrelevant and the coverage probability is given by the following Corollary.

Corollary 1. *Setting $\mathcal{K}_1 = \emptyset$, coverage probability for TYPE 1 is given by:*

$$P_c = \sum_{i \in \mathcal{K}_2} 2\pi \lambda_i \int_0^\infty \exp\left(-\frac{\tau_i N_0 r^\alpha}{P_i}\right) \exp\left(-\pi r^2 \sum_{j \in \mathcal{K}_2} \lambda_j \bar{P}_{j,i}^2 \rho(\tau_i, \alpha)\right) r dr, \quad (20)$$

and, for interference-limited networks ($N_0 = 0$),

$$P_c = \frac{\sum_{i \in \mathcal{K}_2} \lambda_i P_i^{\frac{2}{\alpha}}}{\sum_{j \in \mathcal{K}_2} \lambda_j P_j^{\frac{2}{\alpha}} \rho(\tau_i, \alpha)}. \quad (21)$$

Proof: This result can be obtained directly from (18b) by setting $\mathcal{K}_1 = \emptyset$. See [12], [31] for the intermediate steps between (20) and (21). \blacksquare

D. Special Cases: TCP and MCP

For the purpose of numerical evaluation of coverage probability, we assume that Φ_k is either a TCP or an MCP which are defined as follows.

Definition 4 (Thomas Cluster Process). *A PCP $\Phi_k(\lambda_{p_k}, g_k, \bar{m}_k)$ is called a TCP if the distribution of the offspring points in \mathcal{B}_k^z is Gaussian around the cluster center at the origin, i.e. for all $\mathbf{s} \in \mathcal{B}_k^z$, if $\mathbf{s} = (\|\mathbf{s}\|, \arg(\mathbf{s})) \equiv (s, \theta_s) \in \mathcal{B}_k^z$ denotes a point of the offspring point process \mathcal{B}_k^z with cluster center at origin,*

$$g_k(\mathbf{s}) = g_k(s, \theta_s) = \frac{s}{\sigma_k^2} \exp\left(-\frac{s^2}{2\sigma_k^2}\right) \frac{1}{2\pi}, \quad s \geq 0, 0 < \theta_s \leq 2\pi. \quad (22)$$

Definition 5 (Matérn Cluster Process). *A PCP $\Phi_k(\lambda_{p_k}, g_k, \bar{m}_k)$ is called an MCP if the distribution of the offspring points in \mathcal{B}_k^z is uniform within a disc of radius r_{d_k} around the origin denoted by $b(\mathbf{0}, r_{d_k})$. Hence,*

$$g_k(\mathbf{s}) = g_k(s, \theta_s) = \frac{2s}{r_{d_k}^2} \times \frac{1}{2\pi}, \quad 0 \leq s \leq r_{d_k}, 0 < \theta_s \leq 2\pi. \quad (23)$$

We now provide the conditional distance distributions of TCP and MCP. When Φ_k is a TCP, given that \mathbf{z} is the cluster center of \mathbf{x} , i.e., $\mathbf{x} \in \mathbf{z} + \mathcal{B}_k^{\mathbf{z}}$, we can write the conditional PDF of x as [41]:

$$f_{d_k}(x|z) = \frac{x}{\sigma_k^2} \exp\left(-\frac{x^2 + z^2}{2\sigma_k^2}\right) I_0\left(\frac{xz}{\sigma_k^2}\right), \quad x, z \geq 0, \quad (24)$$

where $I_0(\cdot)$ is the modified Bessel function of the first kind with order zero, and,

$$f_{d_k}(x|0) = \frac{x}{\sigma_k^2} \exp\left(-\frac{x^2}{2\sigma_k^2}\right), \quad x \geq 0. \quad (25)$$

When Φ_k is an MCP, $f_{d_k}(x|z) = \chi_k^{(\ell)}(x, z)$, ($\ell = 1, 2$), where

$$\chi_k^{(1)}(x, z) = \frac{2x}{r_{d_k}^2}, \quad 0 \leq x \leq r_{d_k} - z, 0 \leq z \leq r_{d_k}, \quad (26a)$$

$$\chi_k^{(2)}(x, z) = \frac{2x}{\pi r_{d_k}^2} \cos^{-1}\left(\frac{x^2 + z^2 - r_{d_k}^2}{2xz}\right), \quad |r_{d_k} - z| < x \leq r_{d_k} + z. \quad (26b)$$

IV. RESULTS AND DISCUSSIONS

We now numerically evaluate the expressions of P_c derived in Theorems 1 and 2. For the numerical evaluation, we choose a two tier network ($K = 2$) with one tier of sparsely deployed MBSs and another tier of densely deployed SBSs. The SBSs are distributed as a PCP and the MBSs are distributed as a PPP, i.e., $\mathcal{K}_1 = \{1\}$ and $\mathcal{K}_2 = \{2\}$. We assume that the network is interference limited ($N_0 = 0$) and the downlink transmit powers of each BS in Φ_1 and Φ_2 are set such that $P_2/P_1 = 10^3$. Also, Φ_1 is assumed to be denser than Φ_2 , i.e., $\bar{m}_1\lambda_{p_1} > \lambda_2$. We also assume $\alpha = 4$ and $\tau_1 = \tau_2 = \tau$. We first verify the analytical results presented in Theorems 1 and 2 with Monte Carlo simulations of the network, for which we set $\bar{m} = 10$, $\lambda_{p_1} = 100 \text{ km}^{-2}$ and $\lambda_2 = 1 \text{ km}^{-2}$. The values of P_c for different values of τ from simulation and analysis are plotted in Fig. 2, where Fig. 2(a) and 2(b) corresponds to Φ_1 being TCP and MCP, respectively. The perfect match between simulation and analytical results, indicated by small circles and curves, respectively, verifies the accuracy of our analysis.

A. Variation of Cluster Size

In Fig. 2, P_c is plotted for different cluster sizes of Φ_1 . The cluster size precisely refers to σ_1 when Φ_1 is a TCP (in Fig. 2(a)) and r_{d_1} when Φ_1 is an MCP (in Fig. 2(b)). We observe that the cluster size has a conflicting effect on P_c : for TYPE 1, P_c increases with cluster size and for

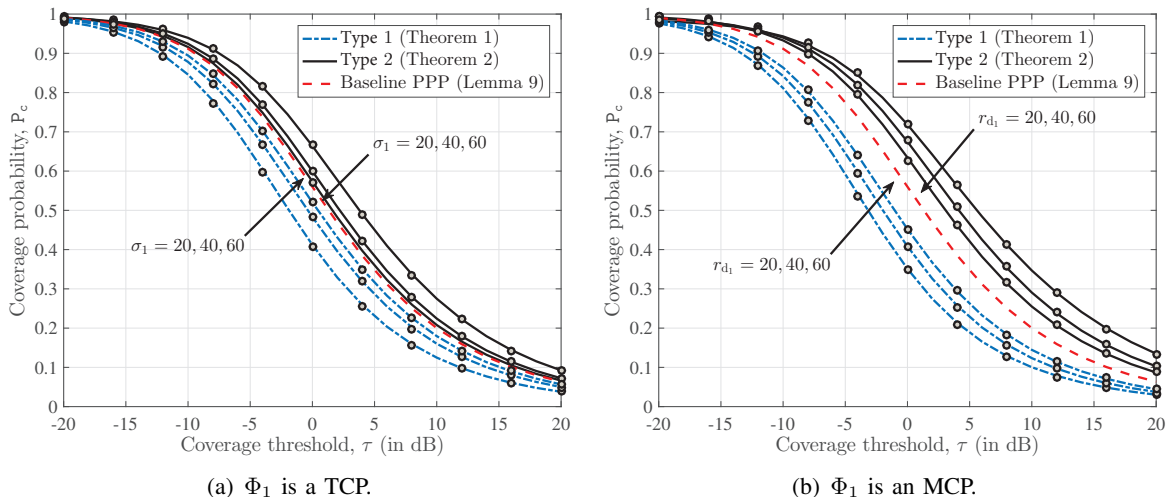


Fig. 2. Coverage probability as a function of SIR threshold ($\alpha = 4$, $P_2 = 10^3 P_1$, $\lambda_2 = 10^{-6} \text{ m}^{-2}$, $\lambda_{p_1} = 10^{-4} \text{ m}^{-2}$, and $\bar{m} = 10$).

TYPE 2, P_c decreases with cluster size. This can be explained as follows. In TYPE 2, due to the spatial coupling between Φ_1 and Φ_u , the candidate serving BS of Φ_1 is more likely to belong to the representative cluster (i.e., the BS cluster with the cluster center of the typical user) and as cluster size increases, this candidate serving BS moves farther away from the user on average. On the other hand, for TYPE 1, as cluster size increases, the BSs of Φ_1 on average lie closer to the typical user. This phenomenon is the consequence of the spatial coupling between BSs and users and is also observed for the max-SINR based association strategy in the similar setup [1]. For both types, as cluster size increases, P_c converges to the coverage probability for a two tier network with both BS tiers being modeled as PPP, more precisely, $\mathcal{K}_1 = \emptyset$, $\mathcal{K}_2 = \{1, 2\}$, with intensities $\lambda_1 = \bar{m}_1 \lambda_{p_1}$ and λ_2 , respectively. The reason for this convergence is the fact that as cluster size tends to infinity, the limiting distribution of a PCP is a PPP [37]. Since the trends of P_c are very similar for Φ_1 being TCP and MCP, we set Φ_1 as TCP for the rest of the discussion.

Another interesting observation from Fig. 2 is that the variation of P_c with cluster size is not as prominent for TYPE 2 as it is for TYPE 1. For further investigation, we focus on the scenario where Φ_1 is a TCP, fix $\tau = 0$ dB and plot the variation of P_c with σ_1 in Fig. 3. We observe that the P_c versus σ_1 curves for TYPE 2 are almost flat. The reason can be explained as follows. For TYPE 2, as cluster size is increased, the nearest BS of Φ_1 belonging to the representative cluster lies farther away while the nearest BS of Φ_1 which does not belong to the representative cluster comes closer. Also, as cluster size increases, the intra-cluster interference,

i.e., the aggregate interference from the BSs of the representative cluster decreases while the inter-cluster interference, i.e., the aggregate interference from the BSs of Φ_1 except the representative cluster increases. Due to these conflicting effects, the cluster size variation do not impact P_c strongly for TYPE 2. On the other hand, for TYPE 1 these conflicts are not present because Φ_u and Φ_1 are not coupled and hence there is no representative BS cluster.

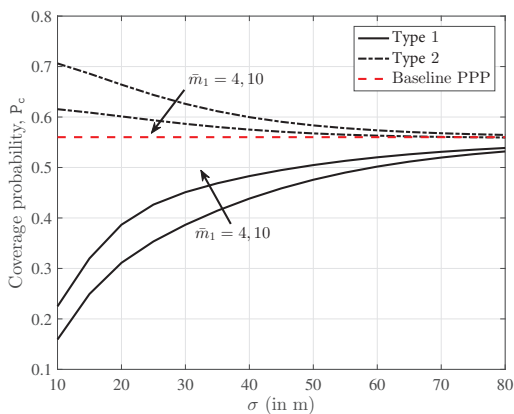


Fig. 3. Coverage probability as a function of σ_1 ($\alpha = 4$, $P_2 = 10^3 P_1$, $\lambda_{p1} = 10^{-4} \text{ m}^{-2}$, $\lambda_2 = 10^{-6} \text{ m}^{-2}$, and $\tau = 0 \text{ dB}$).

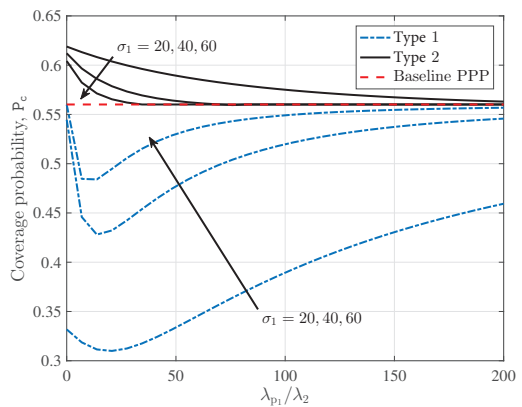


Fig. 4. Coverage probability as a function of λ_{p1}/λ_2 ($\alpha = 4$, $P_2 = 10^3 P_1$, $\tau = 0 \text{ dB}$, and $\bar{m} = 10$).

B. Variation of BS Intensity

We now vary the intensity of the parent PPP (λ_{p1}) keeping λ_2 constant and plot the coverage probability in Fig. 4. For an interference-limited HetNet with the same SIR threshold for all tiers, it is a well-known result that if the BSs are modeled as PPPs, P_c is independent of the BS intensity. This can be readily verified by putting $\tau_i = \tau \forall i$ in (21) which yields $P_c = 1/\rho(\tau, \alpha)$. However, once the spatial distribution of BSs is changed to PCP, we see that P_c is rather strongly dependent on the BS intensity under similar set of assumptions. From Fig. 4, we also observe that for large values of λ_{p1} , P_c converges to $1/\rho(\tau, \alpha)$, i.e., the coverage when the BSs are modeled as PPPs.

Remark 4. *Although it is difficult to visualize the variation of P_c in the parameter space, which for the two tier network under consideration is $\lambda_{p1} \times \lambda_2 \times \bar{m}_1 \times \sigma_1$, using the results in [42], it is possible to find the trajectories (known as equi-coverage contours) in the parameter space along which P_c remains constant. The family of equicoverage contours are generated by $(\lambda_{p1}/l^2, \lambda_2/l^2, \sigma_1 l)$ where $l > 0$ is a scalar. When Φ_1 is an MCP, a similar result can be obtained*

by replacing σ_1 by r_{d_1} .

V. CONCLUSION

Although it is more realistic to model BS and user locations of a HetNet as PCPs, the exact characterization of coverage probability for the max-power based association strategy for PCP distributed BSs has remained an open problem for a while. The main contribution of this paper is a concrete resolution of this problem. In particular, we developed an analytical framework for evaluating the coverage probability of a typical user in a K -tier HetNet model where the locations of a fraction of BS tiers are modeled as PCP and the rest are modeled as PPP. To be consistent with 3GPP HetNet models, we also assumed that the user distribution is either independent of or spatially coupled to the BS distribution. This work, along with our previous work [1] (focused on max-SINR based association), provides a complete characterization of downlink coverage probability in the unified HetNet model, which is an important generalization of the well-known baseline PPP-based model.

This work has numerous extensions. An immediate extension is to study other key performance metrics such as rate coverage probability and percentile rates which will take into account the distributions of load or the number of users connected to the BSs. From stochastic geometry perspective, this will necessitate characterizing the Voronoi cells generated by PCP-distributed BSs whose properties are not well-studied in the literature. From a modeling perspective, another extension is to incorporate more realistic channel models including shadowing, blocking and general pathloss, e.g. in the context of millimeter wave (mm-wave) communication. Especially for mm-wave integrated access and backhaul (IAB) in 5G [43], the PCP is a natural candidate for modeling the locations of the SBSs forming clusters around the MBS that provides wireless backhaul over mmWave links. More generally, the framework developed in this paper will lay the foundation to the performance analysis of such networks where the spatial coupling between the BS and user locations cannot be ignored.

APPENDIX

A. Proof of Lemma 3

When $i \in \mathcal{K}_1$,

$$\mathbb{P}(\mathcal{S}_i | \Phi_{p_k}, \forall k \in \mathcal{K}_1) = \mathbb{P} \left(\bigcap_{j \in \mathcal{K} \setminus \{i\}} P_i \|\tilde{\mathbf{x}}_i\|^{-\alpha} > P_j \|\tilde{\mathbf{x}}_j\|^{-\alpha} \middle| \Phi_{p_k}, \forall k \in \mathcal{K}_1 \right)$$

$$\begin{aligned}
&= \prod_{j_1 \in \mathcal{K}_1 \setminus \{i\}} \mathbb{P} \left(\|\tilde{\mathbf{x}}_{j_1}\| > \left(\frac{P_{j_1}}{P_i}\right)^{1/\alpha} \|\tilde{\mathbf{x}}_i\| \middle| \Phi_{p_i}, \Phi_{p_{j_1}} \right) \prod_{j_2 \in \mathcal{K}_2} \mathbb{P} \left(\|\tilde{\mathbf{x}}_{j_2}\| > \left(\frac{P_{j_2}}{P_i}\right)^{1/\alpha} \|\tilde{\mathbf{x}}_i\| \middle| \Phi_{p_i} \right) \\
&\stackrel{(a)}{=} \int_0^\infty \prod_{j_1 \in \mathcal{K}_1 \setminus \{i\}} \bar{F}_{c_{j_1}} \left(\left(\frac{P_{j_1}}{P_i}\right)^{1/\alpha} r \middle| \Phi_{p_{j_1}} \right) \prod_{j_2 \in \mathcal{K}_2} \bar{F}_{c_{j_2}} \left(\left(\frac{P_{j_2}}{P_i}\right)^{1/\alpha} r \right) f_{c_i}(r | \Phi_{p_i}) dr \\
&\stackrel{(b)}{=} \int_0^\infty \prod_{j_1 \in \mathcal{K}_1 \setminus \{i\}} \prod_{\mathbf{z} \in \Phi_{p_{j_1}}} \exp \left(-\bar{m}_{j_1} F_{d_{j_1}} \left(\left(\frac{P_{j_1}}{P_i}\right)^{1/\alpha} r \middle| z \right) \right) \prod_{j_2 \in \mathcal{K}_2} \exp \left(-\pi \lambda_{j_2} \left(\frac{P_{j_2}}{P_i}\right)^{2/\alpha} r^2 \right) \times \\
&\quad \bar{m}_i \sum_{\mathbf{z} \in \Phi_{p_i}} f_{d_i}(r|z) \prod_{\mathbf{z} \in \Phi_{p_i}} \exp(-\bar{m}_i F_{d_i}(r|z)) dr \\
&= \bar{m}_i \int_0^\infty \sum_{\mathbf{z} \in \Phi_{p_i}} f_{d_i}(r|z) \prod_{j_1 \in \mathcal{K}_1} \prod_{\mathbf{z} \in \Phi_{p_{j_1}}} \exp \left(-\bar{m}_{j_1} F_{d_{j_1}} \left(\left(\frac{P_{j_1}}{P_i}\right)^{1/\alpha} r \middle| z \right) \right) \exp \left(-\pi \sum_{j_2 \in \mathcal{K}_2} \lambda_{j_2} \left(\frac{P_{j_2}}{P_i}\right)^{2/\alpha} r^2 \right) dr.
\end{aligned}$$

Here (a) follows from the fact that Φ_i -s are independent, (b) follows from Lemma 2, and $\bar{F}_{c_j}(\cdot)$ denotes the complementary CDF (CCDF) of $\|\tilde{\mathbf{x}}_j\|$. When $i \in \mathcal{K}_2$,

$$\begin{aligned}
&\mathbb{P}(\mathcal{S}_i | \Phi_{p_k}, \forall k \in \mathcal{K}_1) \\
&= \prod_{j_1 \in \mathcal{K}_1} \mathbb{P} \left(\|\tilde{\mathbf{x}}_{j_1}\| > \left(\frac{P_{j_1}}{P_i}\right)^{1/\alpha} \|\tilde{\mathbf{x}}_i\| \middle| \Phi_{p_{j_1}} \right) \prod_{j_2 \in \mathcal{K}_2 \setminus \{i\}} \mathbb{P} \left(\|\tilde{\mathbf{x}}_{j_2}\| > \left(\frac{P_{j_2}}{P_i}\right)^{1/\alpha} \|\tilde{\mathbf{x}}_i\| \right) \\
&= \int_0^\infty \prod_{j_1 \in \mathcal{K}_1} \bar{F}_{c_{j_1}} \left(\left(\frac{P_{j_1}}{P_i}\right)^{1/\alpha} r \middle| \Phi_{p_{j_1}} \right) \prod_{j_2 \in \mathcal{K}_2 \setminus \{i\}} \bar{F}_{c_{j_2}} \left(\left(\frac{P_{j_2}}{P_i}\right)^{1/\alpha} r \right) f_{c_i}(r) dr \\
&= 2\pi \lambda_i \int_0^\infty \prod_{j_1 \in \mathcal{K}_1} \prod_{\mathbf{z} \in \Phi_{p_{j_1}}} \exp \left(-\bar{m}_{j_1} F_{d_{j_1}} \left(\left(\frac{P_{j_1}}{P_i}\right)^{1/\alpha} r \middle| z \right) \right) \exp \left(-\pi \sum_{j_2 \in \mathcal{K}_2} \lambda_{j_2} \left(\frac{P_{j_2}}{P_i}\right)^{2/\alpha} r^2 \right) r dr,
\end{aligned}$$

where the last step follows from Lemma 2.

B. Proof of Lemma 4

The conditional CCDF of $\|\mathbf{x}^*\|$ given \mathcal{S}_i and $\Phi_{p_k}, \forall k \in \mathcal{K}_1$: is given by:

$$\begin{aligned}
\bar{F}_{s_i}(r | \mathcal{S}_i, \Phi_{p_k}, \forall k \in \mathcal{K}_1) &= \mathbb{P}(\|\mathbf{x}^*\| > r | \mathcal{S}_i, \Phi_{p_k}, \forall k \in \mathcal{K}_1) = \mathbb{P}(\|\tilde{\mathbf{x}}_i\| > r | \mathcal{S}_i, \Phi_{p_k}, \forall k \in \mathcal{K}_1) \\
&= \frac{\mathbb{P}(\|\tilde{\mathbf{x}}_i\| > r, \mathcal{S}_i | \Phi_{p_k}, \forall k \in \mathcal{K}_1)}{\mathbb{P}(\mathcal{S}_i | \Phi_{p_k}, \forall k \in \mathcal{K}_1)}.
\end{aligned}$$

Now

$$\mathbb{P}(\|\tilde{\mathbf{x}}_i\| > r, \mathcal{S}_i | \Phi_{p_k}, \forall k \in \mathcal{K}_1) = \mathbb{P} \left(\prod_{j \in \mathcal{K} \setminus \{i\}} P_j \|\tilde{\mathbf{x}}_j\|^{-\alpha} > P_j \|\tilde{\mathbf{x}}_j\|^{-\alpha}, \|\tilde{\mathbf{x}}_i\| > r | \Phi_{p_k}, \forall k \in \mathcal{K}_1 \right).$$

This expression is similar to the expression appearing in the computation of association probability with the additional event that $\|\tilde{\mathbf{x}}_i\| > r$ which can be handled by changing the lower limit of the integral in (9). The final step is to differentiate the CCDF with respect to r .

C. Proof of Lemma 7

We first compute the probability of the i^{th} coverage event given $\Phi_{\mathbf{p}_k}, \forall k \in \mathcal{K}_1$ as follows.

$$\mathbb{P}(\text{SINR}(\mathbf{x}^*) > \tau_i, \mathcal{S}_i | \Phi_{\mathbf{p}_k}, \forall k \in \mathcal{K}_1) = \mathbb{P}(\mathcal{S}_i | \Phi_{\mathbf{p}_k}, \forall k \in \mathcal{K}_1) \mathbb{P}(\text{SINR}(\mathbf{x}^*) > \tau_i | \mathcal{S}_i, \Phi_{\mathbf{p}_k}, \forall k \in \mathcal{K}_1),$$

where $\mathbb{P}(\text{SINR}(\mathbf{x}^*) > \tau_i | \mathcal{S}_i, \Phi_{\mathbf{p}_k}, \forall k \in \mathcal{K}_1) =$

$$\begin{aligned} & \mathbb{P} \left(\frac{P_i h_{\mathbf{x}^*} \|\mathbf{x}^*\|^{-\alpha}}{N_0 + \sum_{j \in \mathcal{K}} \sum_{\mathbf{y} \in \Phi_j \setminus \{\mathbf{x}^*\}} P_j h_{\mathbf{y}} \|\mathbf{y}\|^{-\alpha}} > \tau_i \middle| \mathcal{S}_i, \Phi_{\mathbf{p}_k}, \forall k \in \mathcal{K}_1 \right) \\ &= \mathbb{P} \left(h_{\mathbf{x}^*} > \frac{\tau_i \|\mathbf{x}^*\|^\alpha}{P_i} \left(N_0 + \sum_{j \in \mathcal{K}} \sum_{\mathbf{y} \in \Phi_j \setminus \{\mathbf{x}^*\}} P_j h_{\mathbf{y}} \|\mathbf{y}\|^{-\alpha} \right) \middle| \mathcal{S}_i, \Phi_{\mathbf{p}_k}, \forall k \in \mathcal{K}_1 \right) \\ &\stackrel{(a)}{=} \mathbb{E} \left[\exp \left(-\frac{\tau_i \|\mathbf{x}^*\|^\alpha}{P_i} \left(N_0 + \sum_{j \in \mathcal{K}} \sum_{\mathbf{y} \in \Phi_j \setminus \{\mathbf{x}^*\}} P_j h_{\mathbf{y}} \|\mathbf{y}\|^{-\alpha} \right) \right) \middle| \mathcal{S}_i, \Phi_{\mathbf{p}_k}, \forall k \in \mathcal{K}_1 \right] \\ &= \mathbb{E} \left[\exp \left(-\frac{\tau_i N_0 \|\mathbf{x}^*\|^\alpha}{P_i} \right) \prod_{j \in \mathcal{K}} \prod_{\mathbf{y} \in \Phi_j \setminus \{\mathbf{x}^*\}} \exp \left(-\frac{\tau_i P_j h_{\mathbf{y}} \|\mathbf{x}^*\|^\alpha}{P_i \|\mathbf{y}\|^\alpha} \right) \middle| \mathcal{S}_i, \Phi_{\mathbf{p}_k}, \forall k \in \mathcal{K}_1 \right] \\ &\stackrel{(b)}{=} \mathbb{E} \left[\exp \left(-\frac{\tau_i N_0 \|\mathbf{x}^*\|^\alpha}{P_i} \right) \prod_{j \in \mathcal{K}} \prod_{\mathbf{y} \in \Phi_j \setminus \{\mathbf{x}^*\}} \mathbb{E}_{h_{\mathbf{y}}} \left[\exp \left(-\frac{\tau_i P_j h_{\mathbf{y}} \|\mathbf{x}^*\|^\alpha}{P_i \|\mathbf{y}\|^\alpha} \right) \right] \middle| \mathcal{S}_i, \Phi_{\mathbf{p}_k}, \forall k \in \mathcal{K}_1 \right] \\ &\stackrel{(c)}{=} \mathbb{E} \left[\exp \left(-\frac{\tau_i N_0 \|\mathbf{x}^*\|^\alpha}{P_i} \right) \prod_{j \in \mathcal{K}} \prod_{\substack{\mathbf{y} \in \Phi_j \cap \\ b(\mathbf{0}, \bar{P}_{j,i} \|\mathbf{x}^*\|)^c}} \frac{1}{1 + \frac{\tau_i P_j \|\mathbf{x}^*\|^\alpha}{P_i \|\mathbf{y}\|^\alpha}} \middle| \mathcal{S}_i, \Phi_{\mathbf{p}_k}, \forall k \in \mathcal{K}_1 \right] \\ &= \int_0^\infty \exp \left(-\frac{\tau_i N_0 r^\alpha}{P_i} \right) \prod_{j_1 \in \mathcal{K}_1} \mathbb{E}_{\Phi_{j_1}} \left[\prod_{\substack{\mathbf{y} \in \Phi_{j_1} \cap \\ b(\mathbf{0}, \bar{P}_{j_1,i} r)^c}} \frac{1}{1 + \frac{\tau_i P_{j_1} r^\alpha}{P_i \|\mathbf{y}\|^\alpha}} \middle| \Phi_{\mathbf{p}_{j_1}} \right] \times \\ & \quad \prod_{j_2 \in \mathcal{K}_2} \mathbb{E}_{\Phi_{j_2}} \left[\prod_{\substack{\mathbf{y} \in \Phi_{j_2} \cap \\ b(\mathbf{0}, \bar{P}_{j_2,i} r)^c}} \frac{1}{1 + \frac{\tau_i P_{j_2} r^\alpha}{P_i \|\mathbf{y}\|^\alpha}} \right] f_{s_i}(r | \mathcal{S}_i, \Phi_{\mathbf{p}_k}, \forall k \in \mathcal{K}_1) dr \end{aligned}$$

$$\begin{aligned}
&= \int_0^\infty \exp\left(-\frac{\tau_i N_0 r^\alpha}{P_i}\right) \prod_{j_1 \in \mathcal{K}_1} \prod_{\mathbf{z} \in \Phi_{p_{j_1}}} \exp\left(-\int_{\bar{P}_{j_1, ir}}^\infty \bar{m}_{j_1} f_{d_{j_1}}(y|\mathbf{z}) \left(1 - \frac{1}{1 + \frac{\tau_i P_{j_1} r^\alpha}{P_i y^\alpha}}\right) dy\right) \times \\
&\quad \prod_{j_2 \in \mathcal{K}_2} \exp\left(-2\pi \lambda_{j_2} \int_{\bar{P}_{j_2, ir}}^\infty \left(1 - \frac{1}{1 + \frac{\tau_i P_{j_2} r^\alpha}{P_i y^\alpha}}\right) y dy\right) f_{s_i}(r|\mathcal{S}_i, \Phi_{p_k}, \forall k \in \mathcal{K}_1) dr. \quad (26)
\end{aligned}$$

Here (a) follows from the fact that $h_{\mathbf{x}^*} \sim \exp(1)$, (b) follows from the assumption that all links undergo i.i.d. fading, and (c) is justified since in $\Phi_j \setminus \{\mathbf{x}^*\}$, there exists no points inside the disc $b(\mathbf{0}, \bar{P}_{j,i} \|\mathbf{x}^*\|)$, which is known as the *exclusion disc*. In the last step, we use the PGFL of PPP from Lemma 5. When $i \in \mathcal{K}_1$, substituting $f_{s_i}(r|\mathcal{S}_i, \Phi_{p_k}, \forall k \in \mathcal{K}_1)$ from (10a), $\mathbb{P}(\text{SINR}(\mathbf{x}^*) > \tau_i, \mathcal{S}_i | \Phi_{p_k}, \forall k \in \mathcal{K}_1) =$

$$\begin{aligned}
&\bar{m}_i \int_0^\infty \exp\left(-\frac{\tau_i N_0 r^\alpha}{P_i}\right) \times \\
&\quad \prod_{j_1 \in \mathcal{K}_1} \prod_{\mathbf{z} \in \Phi_{p_{j_1}}} \exp\left(-\bar{m}_{j_1} F_{d_{j_1}}(\bar{P}_{j_1, ir} | z) - \bar{m}_{j_1} \int_{\bar{P}_{j_1, ir}}^\infty f_{d_{j_1}}(y|z) \left(1 - \frac{1}{1 + \frac{\tau_i P_{j_1} r^\alpha}{P_i y^\alpha}}\right) dy\right) \times \\
&\quad \exp\left(-2\pi \sum_{j_2 \in \mathcal{K}_2} \lambda_{j_2} \int_{\bar{P}_{j_2, ir}}^\infty \left(1 - \frac{1}{1 + \frac{\tau_i P_{j_2} r^\alpha}{P_i y^\alpha}}\right) y dy - \pi \sum_{j_2 \in \mathcal{K}_2} \lambda_{j_2} \bar{P}_{j_2, ir}^2\right) \sum_{\mathbf{z} \in \Phi_{p_i}} f_{d_i}(r|z) dr \\
&= \bar{m}_i \int_0^\infty \exp\left(-\frac{\tau_i N_0 r^\alpha}{P_i}\right) \prod_{j_1 \in \mathcal{K}_1} \prod_{\mathbf{z} \in \Phi_{p_{j_1}}} \exp\left(-\bar{m}_{j_1} \left(1 - \int_{\bar{P}_{j_1, ir}}^\infty \frac{f_{d_{j_1}}(y|z)}{1 + \frac{\tau_i P_{j_1} r^\alpha}{P_i y^\alpha}} dy\right)\right) \times \\
&\quad \exp\left(-\pi r^2 \sum_{j_2 \in \mathcal{K}_2} \lambda_{j_2} \bar{P}_{j_2, ir}^2 \tau_i^{2/\alpha} \int_{\tau_i^{-2/\alpha}}^\infty \frac{1}{1+t^{\alpha/2}} dt - \pi \sum_{j_2 \in \mathcal{K}_2} \lambda_{j_2} \bar{P}_{j_2, ir}^2\right) \sum_{\mathbf{z} \in \Phi_{p_i}} f_{d_i}(r|z) dr.
\end{aligned}$$

In the last step, we substitute $\frac{\tau_i P_{j_2} r^\alpha}{P_i y^\alpha} = t^{-\alpha/2}$. The final expression is obtained by some algebraic simplification. When $i \in \mathcal{K}_2$, substituting $f_{s_i}(r|\Phi_{p_k}, k \in \mathcal{K}_1)$ in (26) by (10b), we get $\mathbb{P}(\text{SINR}(\mathbf{x}^*) > \tau_i, \mathcal{S}_i | \Phi_{p_k}, \forall k \in \mathcal{K}_1) =$

$$2\pi \lambda_i \int_0^\infty \exp\left(-\frac{\tau_i N_0 r^\alpha}{P_i}\right) \times$$

$$\prod_{j_1 \in \mathcal{K}_1} \prod_{\mathbf{z} \in \Phi_{\mathcal{P}_{j_1}}} \exp \left(-\bar{m}_{j_1} F_{d_{j_1}}(\bar{P}_{j_1, i} r | z) - \bar{m}_{j_1} \int_{\bar{P}_{j_1, i} r}^{\infty} f_{d_{j_1}}(y | z) \left(1 - \frac{1}{1 + \frac{\tau_i P_{j_1} r^\alpha}{P_i y^\alpha}} \right) dy \right) \times$$

$$\exp \left(- \sum_{j_2 \in \mathcal{K}_2} 2\pi \lambda_{j_2} \int_{\bar{P}_{j_2, i} r}^{\infty} \left(1 - \frac{1}{1 + \frac{\tau_i P_{j_2} r^\alpha}{P_i y^\alpha}} \right) y dy - \sum_{j_2 \in \mathcal{K}_2} \pi \lambda_{j_2} r^2 \left(\frac{P_{j_2}}{P_i} \right)^{2/\alpha} \right) r dr.$$

The final expression is obtained by some algebraic simplification.

D. Proof of Theorem 2

When $i \in \mathcal{K}_1 \setminus \{q\}$, $\mathbb{P}(\text{SINR} > \tau_i, \mathcal{S}_i) =$

$$\bar{m}_i \int_0^\infty \exp \left(-\frac{\tau_i N_0 r^\alpha}{P_i} \right) \prod_{j_1 \in \mathcal{K}_1 \setminus \{i, q\}} \mathbb{E}_{\Phi_{\mathcal{P}_{j_1}}} \left[\prod_{\mathbf{z} \in \Phi_{\mathcal{P}_{j_1}}} \mathcal{C}_{j_1, i}(r, z) \right] \times$$

$$\mathbb{E}_{\Phi_{\mathcal{P}_q}} \left[\prod_{\mathbf{z} \in \Phi_{\mathcal{P}_q}} \mathcal{C}_{q, i}(r, z) \right] \exp \left(-\pi r^2 \sum_{j_2 \in \mathcal{K}_2} \lambda_{j_2} \bar{P}_{j_2, i}^2 \rho(\tau_i, \alpha) \right) \mathbb{E}_{\Phi_{\mathcal{P}_i}} \left[\sum_{\mathbf{z} \in \Phi_{\mathcal{P}_i}} f_{d_i}(r | z) \prod_{\mathbf{z} \in \Phi_{\mathcal{P}_i}} \mathcal{C}_{i, i}(r, z) \right] dr.$$

As opposed to TYPE 1, the product over all points of $\Phi_{\mathcal{P}_q}$ has to be handled explicitly. The PGFL of $\Phi_{\mathcal{P}_q}$ for TYPE 2 evaluated at $\mathcal{C}_{q, i}(r, z)$ is given by

$$\mathbb{E} \left[\prod_{\mathbf{z} \in \Phi_{\mathcal{P}_q}} \mathcal{C}_{q, i}(r, z) \right] = \mathbb{E} [\mathcal{C}_{q, i}(r, z_0)] \mathbb{E} \left[\prod_{\mathbf{z} \in \Phi(\lambda_{\mathcal{P}_q})} \mathcal{C}_{q, i}(r, z) \right] = \mathbb{E} [\mathcal{C}_{q, i}(r, z_0)] \times$$

$$\exp \left(-2\pi \lambda_{\mathcal{P}_q} \int_0^\infty (1 - \mathcal{C}_{q, i}(r, z)) z dz \right).$$

This step is enabled by the fact that \mathbf{z}_0 and $\Phi(\lambda_{\mathcal{P}_q})$ are independent. Substituting $\mu(\mathbf{z}) = \mathcal{C}_{q, i}(z, r)$ and proceeding on similar lines of the proof of Theorem 1, we obtain the final expression. Also note that since the function of \mathbf{z}_0 under consideration is only dependent on $\|\mathbf{z}_0\| \equiv z_0$, while taking expectation over \mathbf{z}_0 , it is sufficient to consider the magnitude distribution of \mathbf{z}_0 which is denoted as $f_{d_u}(z_0|0)$. Now when $i = q$,

$$\mathbb{P}(\text{SINR} > \tau_i, \mathcal{S}_i) = \bar{m}_q \int_0^\infty \exp \left(-\frac{\tau_q N_0 r^\alpha}{P_q} \right) \prod_{j_1 \in \mathcal{K}_1 \setminus \{q\}} \mathbb{E}_{\Phi_{\mathcal{P}_{j_1}}} \left[\prod_{\mathbf{z} \in \Phi_{\mathcal{P}_{j_1}}} \mathcal{C}_{j_1, q}(r, z) \right] \times$$

$$\exp \left(-\pi r^2 \sum_{j_2 \in \mathcal{K}_2} \lambda_{j_2} \bar{P}_{j_2, q}^2 \rho(\tau_q, \alpha) \right) \mathbb{E}_{\Phi_{\mathcal{P}_q}} \left[\sum_{\mathbf{z} \in \Phi_{\mathcal{P}_q}} f_{d_q}(r | z) \prod_{\mathbf{z} \in \Phi_{\mathcal{P}_q}} \mathcal{C}_{q, q}(r, z) \right] dr,$$

where the last term in the expression under integral is the sum-product functional over Φ_{p_q} which is computed as:

$$\begin{aligned}
& \mathbb{E}_{\Phi_{p_q}} \left[\sum_{\mathbf{z} \in \Phi_{p_q}} f_{d_q}(r|z) \prod_{\mathbf{z} \in \Phi_{p_q}} \mathcal{C}_{q,q}(r, z) \right] = \mathbb{E} [f_{d_q}(r|z_0) \mathcal{C}_{q,q}(r, z_0)] \mathbb{E}_{\Phi(\lambda_{p_q})} \left[\prod_{\mathbf{z} \in \Phi(\lambda_{p_q})} \mathcal{C}_{q,q}(r, z) \right] \\
& + \mathbb{E}_{\Phi(\lambda_{p_q})} \left[\sum_{\mathbf{z} \in \Phi_{p_q}} f_{d_q}(r|z) \prod_{\mathbf{z} \in \Phi_{p_q}} \mathcal{C}_{q,q}(r, z) \right] \mathbb{E}[\mathcal{C}_{q,q}(r, z_0)] \\
& = \int_0^\infty f_{d_q}(r|z_0) \mathcal{C}_{q,q}(r, z_0) f_{d_u}(z_0|0) dz_0 \exp \left(-2\pi \lambda_{p_q} \int_0^\infty (1 - \mathcal{C}_{q,q}(r, z)) z dz \right) \\
& + 2\pi \lambda_{p_q} \int_0^\infty f_{d_q}(r|z) \mathcal{C}_{q,q}(r, z) z dz \exp \left(-2\pi \lambda_{p_q} \int_0^\infty (1 - \mathcal{C}_{q,q}(r, z)) z dz \right) \int_0^\infty \mathcal{C}_{q,q}(r, z_0) f_{d_u}(z_0|0) dz_0 \\
& = \exp \left(-2\pi \lambda_{p_q} \int_0^\infty (1 - \mathcal{C}_{q,q}(r, z)) z dz \right) \left(\int_0^\infty f_{d_q}(r|z_0) \mathcal{C}_{q,q}(r, z_0) f_{d_u}(z_0|0) dz_0 \right. \\
& \left. + 2\pi \lambda_{p_q} \int_0^\infty f_{d_q}(r|z) \mathcal{C}_{q,q}(r, z) z dz \int_0^\infty \mathcal{C}_{q,q}(r, z_0) f_{d_u}(z_0|0) dz_0 \right).
\end{aligned}$$

The final expression can be obtained by proceeding on similar lines of the proof of Theorem 1.

Now, for $i \in \mathcal{K}_2$, $\mathbb{P}(\text{SINR} > \tau_i, \mathcal{S}_i) =$

$$\begin{aligned}
& 2\pi \lambda_i \int_0^\infty \exp \left(-\frac{\tau_i N_0 r^\alpha}{P_i} \right) \prod_{j_1 \in \mathcal{K}_1 \setminus \{q\}} \mathbb{E}_{\Phi_{p_{j_1}}} \left[\prod_{\mathbf{z} \in \Phi_{p_{j_1}}} \mathcal{C}_{j_1,i}(r, z) \right] \times \\
& \mathbb{E}_{\Phi_{p_q}} \left[\prod_{\mathbf{z} \in \Phi_{p_q}} \mathcal{C}_{q,i}(r, z) \right] \exp \left(-\pi r^2 \sum_{j_2 \in \mathcal{K}_2} \lambda_{j_2} \bar{P}_{j_2,i}^2 \rho(\tau_i, \alpha) \right) r dr.
\end{aligned}$$

Since expression is very similar to the expression of $\mathbb{P}(\text{SINR} > \tau_i, \mathcal{S}_i)$ obtained for $i \in \mathcal{K}_1 \setminus \{q\}$, we omit the next steps leading to the final expression.

REFERENCES

- [1] C. Saha, M. Afshang, and H. S. Dhillon, "3GPP-inspired HetNet model using Poisson cluster process: Sum-product functionals and downlink coverage," *IEEE Trans. on Commun.*, vol. 66, no. 5, pp. 2219–2234, May 2018.
- [2] M. Mirahsan, R. Schoenen, and H. Yanikomeroglu, "HetHetNets: Heterogeneous traffic distribution in heterogeneous wireless cellular networks," *IEEE Journal on Sel. Areas in Commun.*, vol. 33, no. 10, pp. 2252–2265, Oct. 2015.
- [3] Y. Zhong, G. Wang, R. Li, T. Han, X. Ge, and T. Q. Quek, "Effect of spatial and temporal traffic statistics on the performance of wireless networks," 2018, available online: arxiv.org/abs/1804.06754.
- [4] 3GPP TR 36.872 V12.1.0, "3rd generation partnership project; technical specification group radio access network; small cell enhancements for E-UTRA and E-UTRAN - physical layer aspects (release 12)," Tech. Rep., Dec. 2013.

- [5] 3GPP TR 36.932 V13.0.0, “3rd generation partnership project; technical specification group radio access network; scenarios and requirements for small cell enhancements for E-UTRA and E-UTRAN; (release 13),” Tech. Rep., Dec. 2015.
- [6] 3GPP TR 36.814, “Further advancements for E-UTRA physical layer aspects,” Tech. Rep., 2010.
- [7] J. Andrews, F. Baccelli, and R. Ganti, “A tractable approach to coverage and rate in cellular networks,” *IEEE Trans. on Commun.*, vol. 59, no. 11, pp. 3122–3134, 2011.
- [8] H. S. Dhillon, R. K. Ganti, F. Baccelli, and J. G. Andrews, “Modeling and analysis of K -tier downlink heterogeneous cellular networks,” *IEEE Journal on Sel. Areas in Commun.*, vol. 30, no. 3, pp. 550–560, Apr. 2012.
- [9] C. Saha, M. Afshang, and H. S. Dhillon, “Enriched K -tier HetNet model to enable the analysis of user-centric small cell deployments,” *IEEE Trans. on Wireless Commun.*, vol. 16, no. 3, pp. 1593–1608, Mar. 2017.
- [10] P. D. Mankar, G. Das, and S. S. Pathak, “Modeling and coverage analysis of BS-centric clustered users in a random wireless network,” *IEEE Wireless Commun. Letters*, vol. 5, no. 2, pp. 208–211, Apr. 2016.
- [11] M. Afshang and H. S. Dhillon, “Poisson cluster process based analysis of HetNets with correlated user and base station locations,” *IEEE Trans. on Wireless Commun.*, vol. 17, no. 4, pp. 2417–2431, Apr. 2018.
- [12] J. G. Andrews, A. K. Gupta, and H. S. Dhillon, “A primer on cellular network analysis using stochastic geometry,” 2016, available online: arxiv.org/abs/1604.03183.
- [13] H. ElSawy, E. Hossain, and M. Haenggi, “Stochastic geometry for modeling, analysis, and design of multi-tier and cognitive cellular wireless networks: A survey,” *IEEE Commun. Surveys Tuts.*, vol. 15, no. 3, pp. 996–1019, 3th quarter 2013.
- [14] S. Mukherjee, *Analytical Modeling of Heterogeneous Cellular Networks*. Cambridge University Press, 2014.
- [15] H. ElSawy, A. Sultan-Salem, M. S. Alouini, and M. Z. Win, “Modeling and analysis of cellular networks using stochastic geometry: A tutorial,” *IEEE Commun. Surveys Tuts.*, vol. 19, no. 1, pp. 167–203, Firstquarter 2017.
- [16] B. Błaszczyszyn, M. Haenggi, P. Keeler, and S. Mukherjee, *Stochastic geometry analysis of cellular networks*. Cambridge University Press, 2018.
- [17] H. S. Dhillon, R. K. Ganti, and J. G. Andrews, “Modeling non-uniform UE distributions in downlink cellular networks,” *IEEE Wireless Commun. Letters*, vol. 2, no. 3, pp. 339–342, Jun. 2013.
- [18] C. Saha and H. S. Dhillon, “Downlink coverage probability of K -tier HetNets with general non-uniform user distributions,” in *Proc., IEEE Intl. Conf. on Commun. (ICC)*, May 2016.
- [19] E. Turgut and M. C. Gursoy, “Downlink analysis in unmanned aerial vehicle (UAV) assisted cellular networks with clustered users,” *IEEE Access*, vol. 6, pp. 36 313–36 324, May 2018.
- [20] Y. Li, F. Baccelli, J. G. Andrews, T. D. Novlan, and J. C. Zhang, “Modeling and analyzing the coexistence of Wi-Fi and LTE in unlicensed spectrum,” *IEEE Trans. on Wireless Commun.*, vol. 15, no. 9, pp. 6310–6326, Sep. 2016.
- [21] P. Parida, H. S. Dhillon, and P. Nuggehalli, “Stochastic geometry-based modeling and analysis of citizens broadband radio service system,” *IEEE Access*, vol. 5, pp. 7326–7349, 2017.
- [22] A. Guo, Y. Zhong, W. Zhang, and M. Haenggi, “The Gauss–Poisson process for wireless networks and the benefits of cooperation,” *IEEE Trans. on Commun.*, vol. 64, no. 5, pp. 1916–1929, May 2016.
- [23] D. B. Taylor, H. S. Dhillon, T. D. Novlan, and J. G. Andrews, “Pairwise interaction processes for modeling cellular network topology,” in *Proc., IEEE Global Commun. Conf. (GLOBECOM)*, Dec. 2012, pp. 4524–4529.
- [24] N. Miyoshi and T. Shirai, “A cellular network model with Ginibre configured base stations,” *Advances in Applied Probability*, vol. 46, no. 3, pp. 832–845, 2014.
- [25] I. Nakata and N. Miyoshi, “Spatial stochastic models for analysis of heterogeneous cellular networks with repulsively deployed base stations,” *Performance Evaluation*, vol. 78, pp. 7–17, 2014.
- [26] Y. Li, F. Baccelli, H. S. Dhillon, and J. G. Andrews, “Statistical modeling and probabilistic analysis of cellular networks with determinantal point processes,” *IEEE Trans. on Commun.*, vol. 63, no. 9, pp. 3405–3422, Sep. 2015.
- [27] N. Deng, W. Zhou, and M. Haenggi, “Heterogeneous cellular network models with dependence,” *IEEE Journal on Sel. Areas in Commun.*, vol. 33, no. 10, pp. 2167–2181, Oct. 2015.
- [28] Z. Yazdanshenasan, H. S. Dhillon, M. Afshang, and P. H. J. Chong, “Poisson hole process: Theory and applications to wireless networks,” *IEEE Trans. on Wireless Commun.*, vol. 15, no. 11, pp. 7531–7546, Nov. 2016.
- [29] C. Saha, M. Afshang, and H. S. Dhillon, “Poisson cluster process: Bridging the gap between PPP and 3GPP HetNet models,” in *Proc., Information Theory and Applications (ITA)*, 2017.
- [30] V. Suryaprakash, J. Møller, and G. Fettweis, “On the modeling and analysis of heterogeneous radio access networks using a Poisson cluster process,” *IEEE Trans. on Wireless Commun.*, vol. 14, no. 2, pp. 1035–1047, Feb. 2015.
- [31] H. S. Jo, Y. J. Sang, P. Xia, and J. G. Andrews, “Heterogeneous cellular networks with flexible cell association: A comprehensive downlink SINR analysis,” *IEEE Trans. on Wireless Commun.*, vol. 11, no. 10, pp. 3484–3495, Oct. 2012.

- [32] M. Afshang, C. Saha, and H. S. Dhillon, "Nearest-neighbor and contact distance distributions for Thomas cluster process," *IEEE Wireless Commun. Letters*, vol. 6, no. 1, pp. 130–133, Feb. 2017.
- [33] —, "Nearest-neighbor and contact distance distributions for Matérn cluster process," *IEEE Commun. Letters*, vol. 21, no. 12, pp. 2686–2689, Dec. 2017.
- [34] W. Bao and B. Liang, "Handoff rate analysis in heterogeneous wireless networks with Poisson and Poisson cluster patterns," in *Proc. 16th ACM International Symposium on Mobile Ad Hoc Networking and Computing*, ser. MobiHoc '15. New York, NY, USA: ACM, 2015, pp. 77–86.
- [35] S. M. Azimi-Abarghouyi, B. Makki, M. Haenggi, M. Nasiri-Kenari, and T. Svensson, "Stochastic geometry modeling and analysis of single- and multi-cluster wireless networks," *IEEE Trans. on Commun.*, vol. 66, no. 10, pp. 4981–4996, Oct. 2018.
- [36] N. Miyoshi, "Downlink coverage probability in cellular networks with Poisson-Poisson cluster deployed base stations," *IEEE Wireless Commun. Letters*, 2018, to appear.
- [37] S. N. Chiu, D. Stoyan, W. S. Kendall, and J. Mecke, *Stochastic Geometry and its Applications*, 3rd ed. New York: John Wiley and Sons, 2013.
- [38] H. S. Dhillon, R. K. Ganti, and J. G. Andrews, "Load-aware modeling and analysis of heterogeneous cellular networks," *IEEE Trans. on Wireless Commun.*, vol. 12, no. 4, pp. 1666–1677, Apr. 2013.
- [39] S. Singh, H. S. Dhillon, and J. G. Andrews, "Offloading in heterogeneous networks: Modeling, analysis, and design insights," *IEEE Trans. on Wireless Commun.*, vol. 12, no. 5, pp. 2484–2497, May. 2013.
- [40] U. Schilcher, S. Toumpis, M. Haenggi, A. Crismani, G. Brandner, and C. Bettstetter, "Interference functionals in Poisson networks," *IEEE Trans. on Inf. Theory*, vol. 62, no. 1, pp. 370–383, Jan. 2016.
- [41] M. Afshang, H. S. Dhillon, and P. H. J. Chong, "Modeling and performance analysis of clustered device-to-device networks," *IEEE Trans. on Wireless Commun.*, vol. 15, no. 7, pp. 4957–4972, Jul. 2016.
- [42] M. Afshang, C. Saha, and H. S. Dhillon, "Equi-coverage contours in cellular networks," *IEEE Wireless Commun. Letters*, vol. 7, no. 5, pp. 700–703, Oct. 2018.
- [43] C. Saha, M. Afshang, and H. S. Dhillon, "Bandwidth partitioning and downlink analysis in millimeter wave integrated access and backhaul for 5G," *IEEE Trans. on Wireless Commun.*, 2018, to appear.